

## **ABSTRACT**

The objective of this paper is to design, simulate and check the performance analysis using experimental setup of a DGS (Defected Ground Structure) low profile printed microstrip patch antenna for multiband 5G wireless applications. The design is made using FR4 epoxy substrate on the HFSS (High Frequency Structure Simulator) software with a compact size of  $8 \times 9 \text{ mm}^2$  with operating frequencies 10.5GHz, 26.11GHz and 50.5GHz and the second design at 21.6 GHz, 26.11 GHz and 50.5 GHz. The relative dielectric permittivity and the thickness of the substrate are 4.4 and 1.4mm. Main motive of this research is to analyse the performance of the designed antenna in terms of gain, return loss, VSWR (Voltage Standing Wave Ratio) and radiation pattern. The DGS is utilized for bandwidth improvement and for decreasing interference in the communication system for 5G. This is done due to increased demand of consumer for services requiring high data rates (greater than 10Gbps). Simulation results show that such antennas can be used effectively since they are light weight, low in volume and requires low fabrication cost and this is also validated by experimental results.

# CHAPTER 1

## 1. INTRODUCTION

In this era of wireless communication, the major challenge which the cellular operators face is, to provide high traffic capacity to the customers [1]. Apart from achieving high data rates, it is also important that a communication network provides wide area coverage and low latency. 5G serves this purpose, since it provides the customers with extraordinary bandwidth availability with unlimited up gradation possibilities. It prompts spectrum harmonization which incorporates encouraging economies of scale, empowering worldwide meandering, lessening hardware plan multifaceted nature, safeguarding battery life, improving spectrum effectiveness and possibly diminishing cross fringe obstruction [2, 3].

For 5G applications, microstrip patch antennas are profoundly prescribed as they are low-profile, light-weight, involve low fabrication cost and has capacity of working over multiple frequency bands and being patch in the meantime adds to its planar structure [4, 5]. But the limitation is its narrow bandwidth which can be overcome by using slotted patch antennas [6, 7, 8]. Significant efforts are made to lead to the miniaturisation of such antennas with robust construct and without compromising with its capabilities [9].

The main motive of this paper is to design a concave rectangular shaped microstrip patch antenna using low cost FR4 substrate and coaxial feed line which is based on CMOS technology for simultaneous use of mobile phones using 5G network and to avoid shortage of bandwidth [10].

In this paper, a simple low profile microstrip patch antenna is proposed which is designed to perform at 10.5GHz, 26.11GHz and 50.5GHz frequencies. Simulations are analysed in terms of gain, VSWR, return loss and radiation pattern and shows promising results [11]. After fabrication, the physically obtained designed antenna is subjected to vector network analyser and anechoic chamber testing for a frequency of 10.5GHz, 26.11GHz and 50.5 GHz for obtaining further results experimentally. The designed antenna will then be capable of:

- ✓ Operating at frequencies in the range of GHz which is considered to be good enough for the 5G operation of mobile handset.

- ✓ Achieving flexibility and reduced cost with effective communication.
- ✓ Reduction in radiation losses due to thin design and high dielectric constant of the substrate.[2]

## **1.1 Microstrip Antenna**

Also known as a printed antenna usually means an antenna fabricated using microstrip techniques on a printed circuit board (PCB)[20]. It is a kind of internal antenna. They are mostly used at microwave frequencies. An individual microstrip antenna consists of a patch of metal foil of various shapes (a patch antenna) on the surface of a PCB (printed circuit board), with a metal foil ground plane on the other side of the board. Most microstrip antennas consist of multiple patches in a two-dimensional array [21]. The antenna is usually connected to the transmitter or receiver through foil microstrip transmission lines. The radio frequency current is applied (or in receiving antennas the received signal is produced) between the antenna and ground plane. Microstrip antennas have become very popular in recent decades due to their thin planar profile which can be incorporated into the surfaces of consumer products, aircraft and missiles; their ease of fabrication using printed circuit techniques; the ease of integrating the antenna on the same board with the rest of the circuit, and the possibility of adding active devices such as microwave integrated circuits to the antenna itself to make active antennas [20].

### **1.1.1 Patch antenna**

The most common type of microstrip antenna is the patch antenna. Antennas using patches as constitutive elements in an array are also possible. A patch antenna is a narrowband, wide-beam antenna fabricated by etching the antenna element pattern in metal trace bonded to an insulating dielectric substrate, such as a printed circuit board, with a continuous metal layer bonded to the opposite side of the substrate which forms a ground plane. Common microstrip antenna shapes are square, rectangular, circular and elliptical, but any continuous shape is possible [20, 21, 22].

### **1.1.2 Advantages**

Microstrip antennas are relatively inexpensive to manufacture and design because of the simple 2-dimensional physical geometry [20]. They are usually employed at UHF and higher frequencies because the size of the antenna is directly tied to the wavelength at the resonant frequency. A single patch antenna provides a maximum directive gain of around 6-9 dB. It is relatively easy to print an array of patches on a single (large) substrate using lithographic techniques [1].

### 1.1.3 Limitations and disadvantages of the MSA

- ✓ Relatively low efficiency (due to dielectric and conductor losses)
- ✓ Low power
- ✓ Spurious feed radiation (surface waves, strips, etc.)
- ✓ Narrow frequency bandwidth (at most a couple of percent)
- ✓ Relatively high level of cross polarization radiation

### 1.1.4 MSA Layers

1. Metallic Patch
2. Substrate
3. Ground

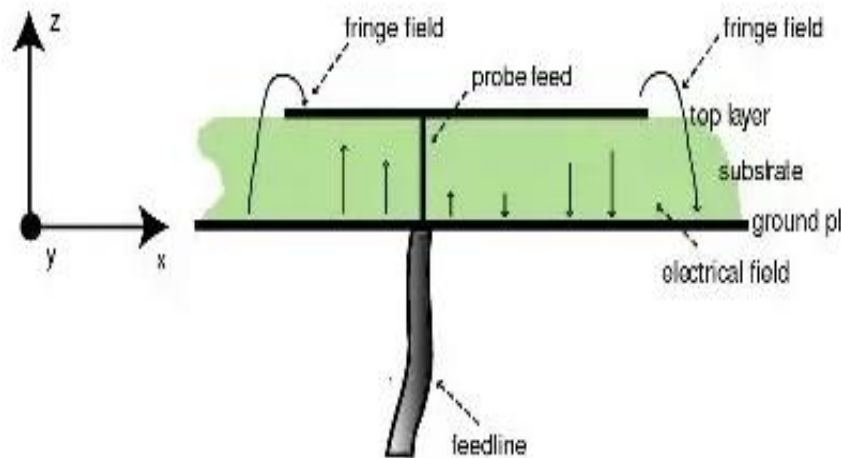


Figure 1: Microstrip Antenna Layers

**Metallic Patch:** Is usually a copper metal which is placed at the top of the substrate and it decides the radiation of the antenna.

**Substrate:** The substrate between patch and ground plane plays important role in design it decides the bandwidth as well as size of the microstrip antenna.

Bandwidth increases with increase in substrate thickness or with decrease in dielectric constant. However there is limit on increasing thickness if increased beyond  $h=0.1$  effective wavelength.

**Ground plane:** As a field reflector and it has a large effect on the radiation patterns and the resonance frequency you could notice that by using numerical methods for analysing your microstrip while most of the analytical methods assume that the ground plane is infinite in size and hence no radiation fields appear in the back of microstrip[22,23].

## 1.2 Fundamental Parameters of Antennas

1. Radiation Pattern
2. Beamwidth
3. Radiation Power Density
4. Radiation Intensity
5. Directivity
6. Antenna Efficiency and Gain
7. Polarization

Important Parameters In order to describe the performance of an antenna, we use various, sometimes interrelated, parameters.

- ✓ Radiation pattern, beamwidth
- ✓ Power
- ✓ Directivity, gain, aperture
- ✓ Radiation resistance

### 1.2.1 Radiation Pattern

An antenna radiation pattern or antenna pattern is defined as a mathematical function or a graphical representation of the radiation properties of the antenna as a function of space coordinates.

- ✓ Defined for the far-field.
- ✓ As a function of directional coordinates.

- ✓ There can be field patterns (magnitude of the electric or magnetic field) or power patterns (square of the magnitude of the electric or magnetic field).
- ✓ Often normalized with respect to their maximum value.
- ✓ The power pattern is usually plotted on a logarithmic scale or more commonly in decibels (dB).

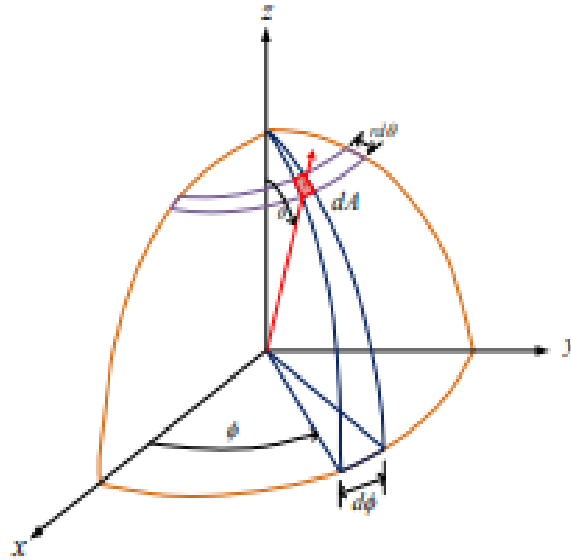


**Figure 2: Radiation patterns are conveniently represented in spherical coordinates**

Pattern:

$$E(\theta, \phi) = d, A = r^2 \sin\theta d\theta d\phi.$$

Azimuth:  $\phi$

Elevation:  $\pi/2 - \theta$ .

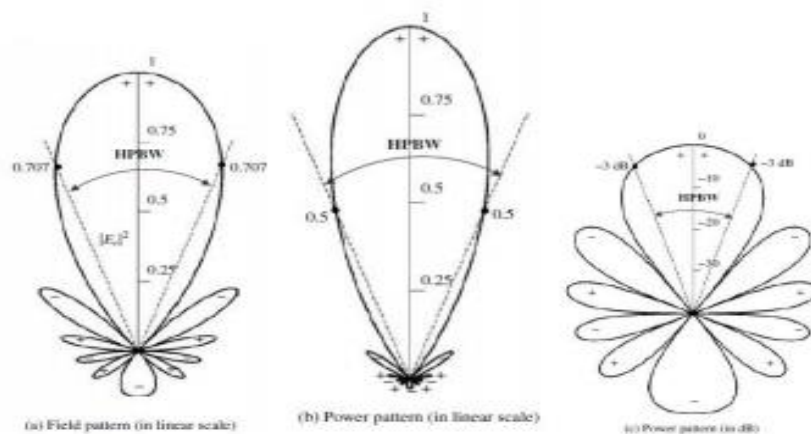


**Figure 3: Field and Power pattern in linear and dB scale**

All three patterns yield the same angular separation between the two half power points,  $38.64^\circ$ , on their respective patterns, referred to as HPBW.

### Radiation Pattern Lobes

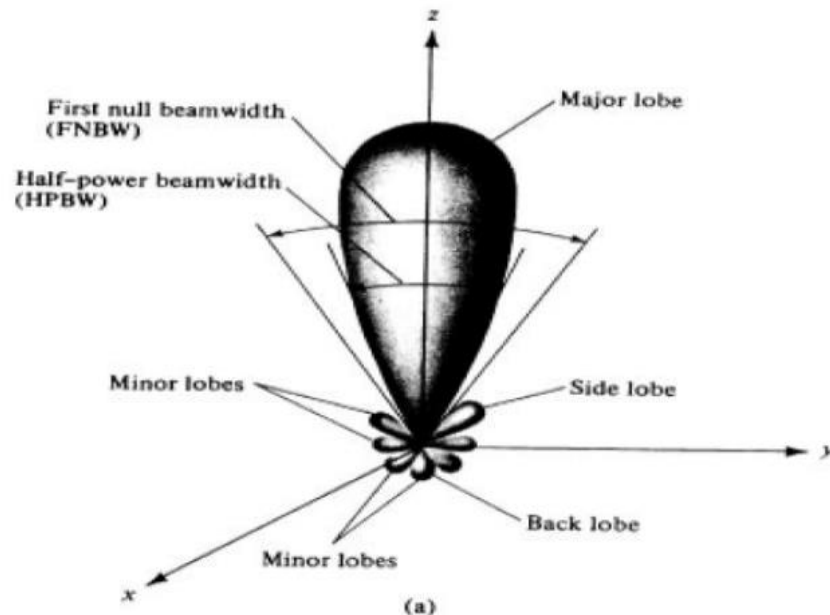


Figure 4: Pattern in spherical co-ordinate system

A radiation lobe is a portion of the radiation pattern bounded by regions of relatively weak radiation intensity.

- ✓ Main lobe
- ✓ Minor lobes
- ✓ Side lobes
- ✓ Back lobes

**Minor lobes:**—Usually represent radiation in undesired directions, and they should be minimized. Side lobes are normally the largest of the minor lobes.

The level of minor lobes is usually expressed as a ratio of the power density, often termed the side lobe ratio or side lobe level.

In most radar systems, low side lobe ratios are very important to minimize false target indications through the side lobes (e.g., -30 dB). Components in the Amplitude Pattern

There would be, in general, three electric-field components ( $E_r$ ,  $E_\theta$ ,  $E_\phi$ ) at each observation point on the surface of a sphere of constant radius.

In the far field, the radial  $E_r$  component for all antennas is zero or vanishingly small. • Some antennas, depending on their geometry and also observation distance, may have only one, two, or all three components[13,14,23].

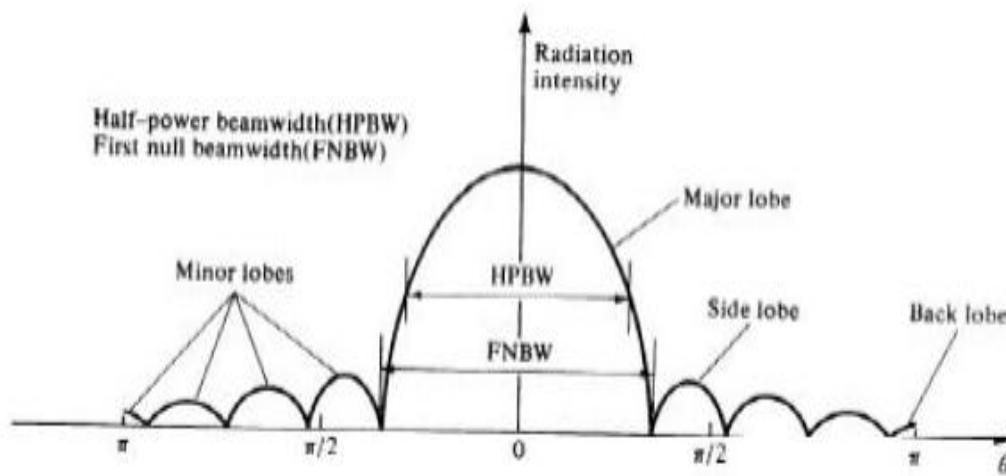


Figure 5: Pattern in Cartesian co-ordinate system

### 1.2.2 Beamwidth

The beamwidth of an antenna is a very important figure of merit and often is used as a trade-off between it and the side lobe level; that is, as the beamwidth decreases, the side lobe increases and vice versa. The beamwidth of the antenna is also used to describe the resolution capabilities of the antenna to distinguish between two adjacent radiating sources or radar targets.

**Half-Power Beam Width (HPBW):-** In a plane containing the direction of the maximum of a beam, the angle between the two directions in which the radiation intensity is one-half value of the beam.

**First-Null Beamwidth (FNBW):-** Angular separation between the first nulls of the pattern.



### Isotropic, Directional, and Omnidirectional Patterns

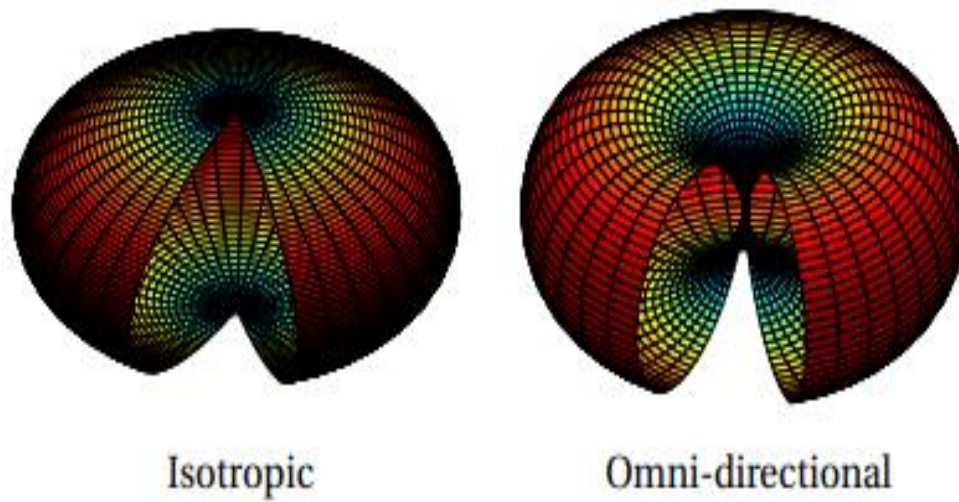


Figure 6: Radiation pattern of Isotropic and Omni-directional antenna

**Omnidirectional Radiator:** - An antenna having an essentially no directional pattern in a given plane (e.g., in azimuth) and a directional pattern in any orthogonal plane.

**Directional Radiator:** - An antenna having the property of radiating or receiving more effectively in some directions than in others. Usually the maximum directivity is significantly greater than that of a half-wave dipole.

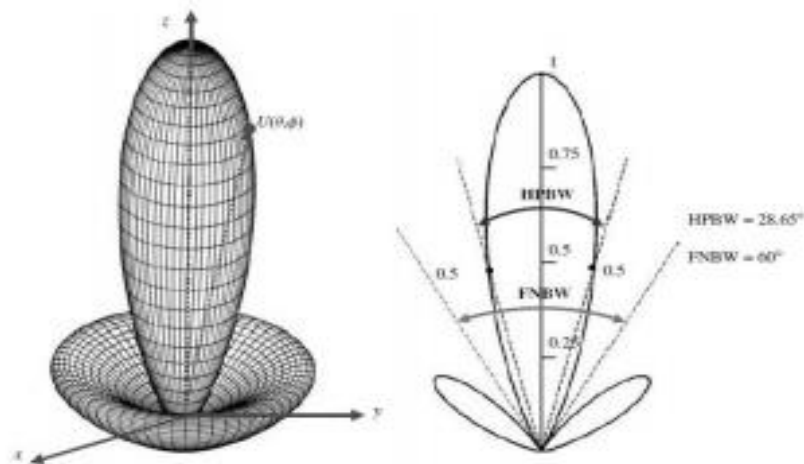


Figure 7: Radiation pattern of antenna

## Resolution

The most common resolution criterion states that the resolution capability of an antenna to distinguish between two sources is equal to half the first-null beamwidth (FNBW/2), which is usually used to approximate the HPBW.

That is, two sources separated by angular distances equal or greater than  $\text{FNBW}/2 \approx \text{HPBW}$  of an antenna with a uniform distribution can be resolved.

If the separation is smaller, then the antenna will tend to smooth the angular separation distance.

The half-power beamwidth HPBW (in radians and degrees). Intensity of an antenna is represented half-power beamwidth HPBW (in radians and degrees) and first-null beamwidth FNBW (in radians and degrees).

## Antenna Fields

### Near- and Far-Fields

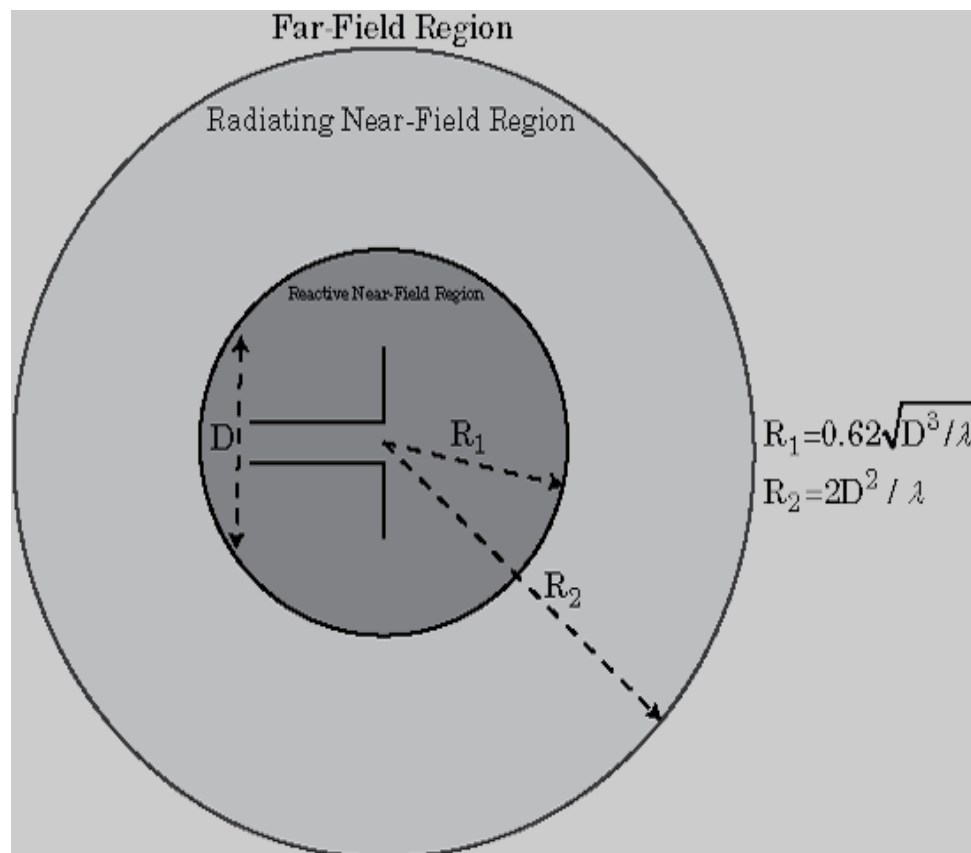


Figure 8: Fields of the antenna

**Reactive near-field region R1:-** The portion of the near-field region immediately surrounding the antenna wherein the reactive field (non-radiating field) predominates.

**Radiating Near-Field (Fresnel) Region:-** The region of the field of an antenna between the reactive near-field region and the far-field region wherein radiation fields predominate and wherein the angular field distribution is dependent upon the distance from the antenna. If the antenna has a maximum dimension that is not large compared to the wavelength, this region may not exist.

**Far-Field (Fraunhofer) Region:-** The region of the field of an antenna where the angular field distribution is essentially independent of the distance from the antenna.

### 1.2.3 Radiation Power Density

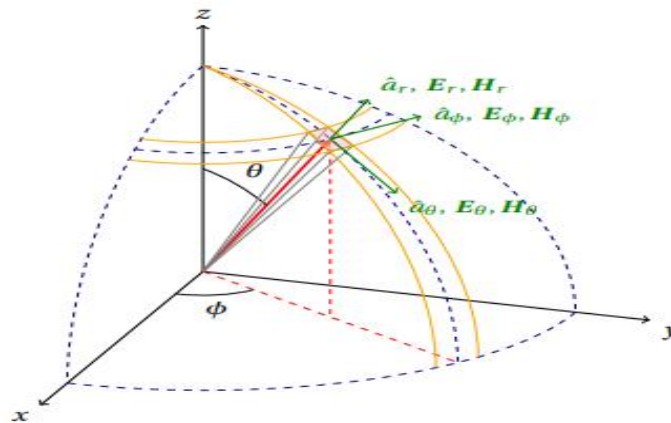


Figure 9: Radiation Power Density in spherical co-ordinate system

### Pointing Vector

The quantity used to describe the power associated with an electromagnetic wave is the instantaneous Pointing vector defined as  $\mathbf{W} = \mathbf{E} \times \mathbf{H}$

Where,

$\mathbf{W}$  = instantaneous Pointing vector (W/m<sup>2</sup>) a power density

$\mathbf{E}$  = instantaneous electric-field intensity (V/m)

$\mathbf{H}$  = instantaneous magnetic-field intensity (A/m)

The total power crossing a closed surface  $P = \oint_S \mathbf{W} \cdot d\mathbf{s} = \oint_S \mathbf{W} \cdot \hat{\mathbf{n}} da$ .

Where

$P$  = instantaneous total power (W)

$\hat{n}$  = unit vector normal to the surface

$a$  = infinitesimal area of the closed surface (m<sup>2</sup>)

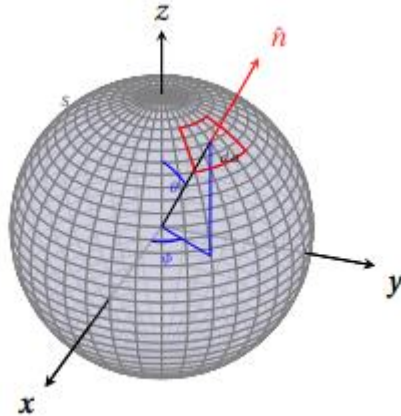


Figure 10: Power Density in spherical co-ordinate system

### Average Power Density

For applications of time-varying fields, it is desirable to find the average power density.

The average power density is obtained by integrating the instantaneous Poynting vector over one period and dividing by the period.

For time-harmonic variations of the form  $e^{j\omega t}$ , we define the complex fields  $E$  and  $H$  which are related to their instantaneous counterparts  $E$  and  $H$  by  $E(x, y, z; t) = \text{Re} [E(x, y, z) e^{j\omega t}]$ ,  $H(x, y, z; t) = \text{Re} [H(x, y, z) e^{j\omega t}]$ .

### Average Radiated Power

The power density associated with the electromagnetic fields of an antenna in its far-field region is predominately real and will be referred to as radiation density.

### Power Pattern versus Average Radiated Power

The power pattern of the antenna is the average power density radiated by the antenna as a function of the direction.

The observations are usually made on a large sphere of constant radius extending into the far field.

In practice, absolute power patterns are usually not desired, but the performance of the antenna is measured in terms of relative power patterns.

Three-dimensional patterns cannot be measured, but they can be constructed with a number of two-dimensional cuts.

#### 1.2.4 Radiation Intensity Steradian

One steradian is defined as the solid angle with its vertex at the center of a sphere of radius  $r$  that is subtended by a spherical surface area equal to that of a square with each side of length  $r$

Since the area of a sphere of radius  $r$  is  $A = 4\pi r^2$ , there are  $4\pi$  sr in a closed sphere.

**Radiation Intensity:** - intensity in a given direction is defined as the power radiated from an antenna per unit solid angle. The radiation intensity is a far-field parameter. It can be obtained by simply multiplying the radiation density by the square of the distance.

$$U = r^2 W_{\text{rad}}.$$

#### 1.2.5 Directivity

The ratio of the radiation intensity in a given direction from the antenna to the radiation intensity averaged over all directions.

**The average radiation intensity:** total power radiated by the antenna divided by  $4\pi$ .

Stated more simply the directivity of a nonisotropic source is equal to the ratio of its radiation intensity in a given direction over that of an isotropic source.

If the direction is not specified, the direction of maximum radiation intensity is implied.

$$D_{\text{max}} = D_0 = U/U_0 = U_{\text{max}}/U_0 = U_{\text{max}}/U_0 = 4\pi U_{\text{max}}/P_{\text{rad}}.$$

$D$  = directivity (dimensionless)

$D_0$  = maximum directivity (dimensionless)

$U = U(\theta, \phi)$  = radiation intensity (W/sr)

$U_{\text{max}}$  = maximum radiation intensity (W/sr)

$U_0$  = radiation intensity of isotropic source (W/sr)

$P_{\text{rad}}$  = total radiated power (W)

### Beam Solid Angle

Beam Solid Angle:- The beam solid angle  $\Omega_A$  is defined as the solid angle through which all the power of the antenna would flow if its radiation intensity is constant (and equal to the maximum value of  $U$ ) for all angles within  $\Omega_A$ .

$$D = 4\pi \Omega_A$$

### 1.2.6 Antenna Efficiency and Gain

The total antenna efficiency  $e_0$  is used to take into account losses at the input terminals and within the structure of the antenna.

$e_0$  is due to the combination of number of efficiencies:  $e_0 = e_r e_c e_d$

$e_0$  = total efficiency,

$e_r$  = reflection (mismatch)

$e_c$  = conduction efficiency

$e_d$  = dielectric efficiency,

$$\Gamma = Z_{in} - Z_0 / Z_{in} + Z_0,$$

$$VSWR = 1 + |\Gamma| / 1 - |\Gamma|.$$

$\Gamma$  = voltage reflection coefficient at the input terminals of the antenna

$Z_{in}$  = antenna input impedance,

$Z_0$  = characteristic impedance of the transmission line.

VSWR = voltage standing wave ratio

Usually  $e_c$  and  $e_d$  are very difficult to compute, but they can be determined experimentally.

#### 1.2.6.1 Gain

The gain of the antenna is closely related to the directivity. In addition to the directional capabilities it accounts for the efficiency of the antenna. Gain does not account for losses arising from impedance mismatches (reflection losses) and polarization mismatches (losses).

Gain the ratio of the intensity in a given direction, to the radiation intensity that would be obtained if the power accepted by the antenna were radiated isotopically.

### Absolute Gain

We can introduce an absolute gain  $G_{abs}$  that takes into account the reflection or mismatch losses (due to the connection of the antenna element to the transmission line

If the antenna is matched to the transmission line, that is, the antenna input impedance  $Z_{in}$  is equal to the characteristic impedance  $Z_c$  of the line ( $|\Gamma| = 0$ ), then the two gains are equal ( $G_{abs} = G$ ). For the maximum values  $G_{0abs} = e_0 D_0$ .

### Bandwidth

For broadband antennas, the bandwidth is usually expressed as the ratio of the upper-to-lower frequencies of acceptable operation. For example, a 10:1 bandwidth indicates that the upper frequency is 10 times greater than the lower.

For narrowband antennas, the bandwidth is expressed as a percentage of the frequency difference (upper minus lower) over the center frequency of the bandwidth. For example, a 5% bandwidth indicates that the frequency difference of acceptable operation is 5% of the center frequency of the bandwidth.

### 1.2.7 Polarization

Polarization is the curve traced by the end point of the arrow (vector) representing the instantaneous electric field. The field must be observed along the direction of propagation.

Polarization is classified as linear, circular, or elliptical.

If the vector that describes the electric field at a point in space as a function of time is always directed along a line, the field is said to be linearly polarized.

In general, the figure that the electric field traces is an ellipse, and the field is said to be elliptically polarized.

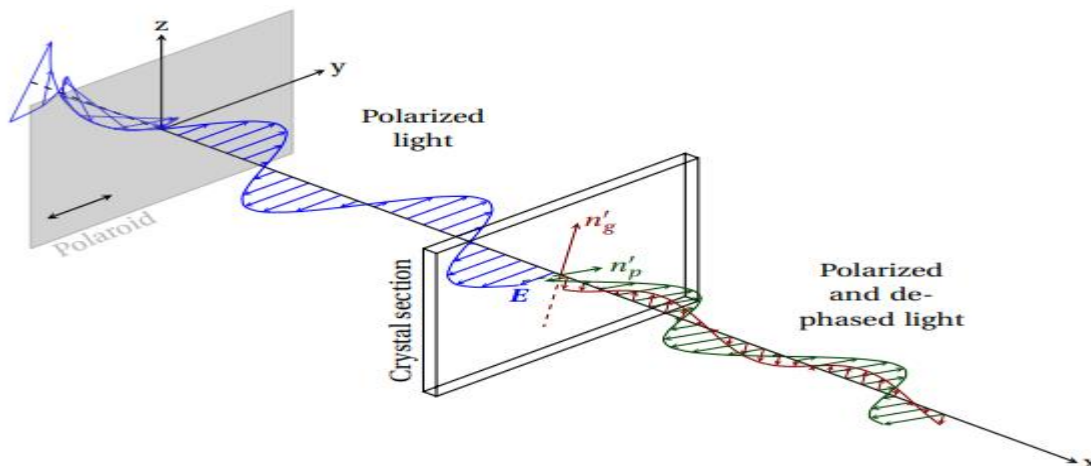


Figure 11: Polarization of the antenna

### Polarized and dephased light Polarization Types

Linear polarization and circular polarization are special cases of elliptic polarization.

Polarization can be clockwise (CW, right-hand polarization), or counter clockwise (CCW, left-hand polarization).

## 1.3 Feeding techniques in microstrip patch antenna

### 1.3.1 Inset Feed:

Previously, the patch antenna was fed at the end as shown in fig 12 since this typically yields a high input impedance, we would like to modify the feed. Since the current is low at the ends of a half-wave patch and increases in magnitude toward the centre, the input impedance ( $Z=V/I$ ) could be reduced if the patch was fed closer to the centre. One method of doing this is by using an inset feed (a distance  $R$  from the end) as shown in Figure 12.

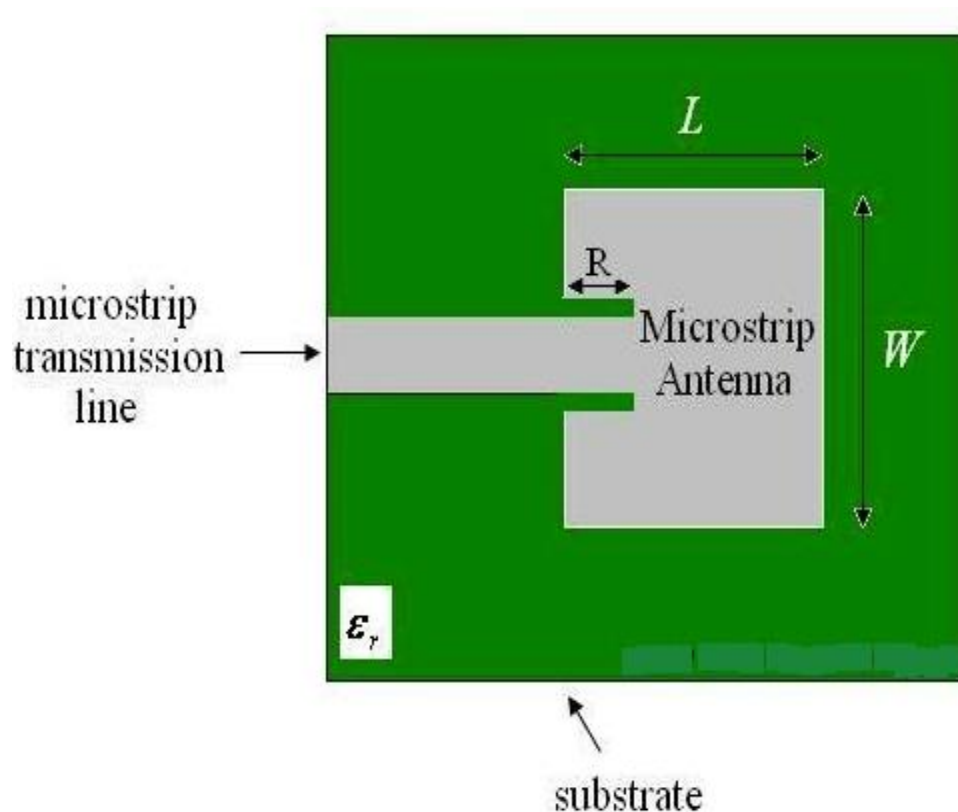


Figure 12: Patch Antenna with an Inset Feed



Since the current has a sinusoidal distribution, moving in a distance  $R$  from the end will increase the current by  $\cos(\pi R/L)$  this is just noting that the wavelength is  $2L$ , and so the phase difference is  $2\pi R/(2L) = \pi R/L$ .

The voltage also decreases in magnitude by the same amount that the current increases. Hence, using  $Z=V/I$ , the input impedance scales as:

$$Z_{in}(R) = \cos^2\left(\frac{\pi R}{L}\right) Z_{in}(0)$$

In the above equation,  $Z_{in}(0)$  is the input impedance if the patch was fed at the end. Hence, by feeding the patch antenna as shown, the input impedance can be decreased. As an example, if  $R=L/4$ , then  $\cos(\pi R/L) = \cos(\pi/4)$ , so that  $[\cos(\pi/4)]^2 = 1/2$ . Hence, a  $(1/8)$ -wavelength inset would decrease the input impedance by 50%. This method can be used to tune the input impedance to the desired value.

### 1.3.2 Fed with a Quarter-Wavelength Transmission Line

The microstrip antenna can also be matched to a transmission line of characteristic impedance  $Z_0$  by using a quarter-wavelength transmission line of characteristic impedance  $Z_1$  as shown in Figure 13.

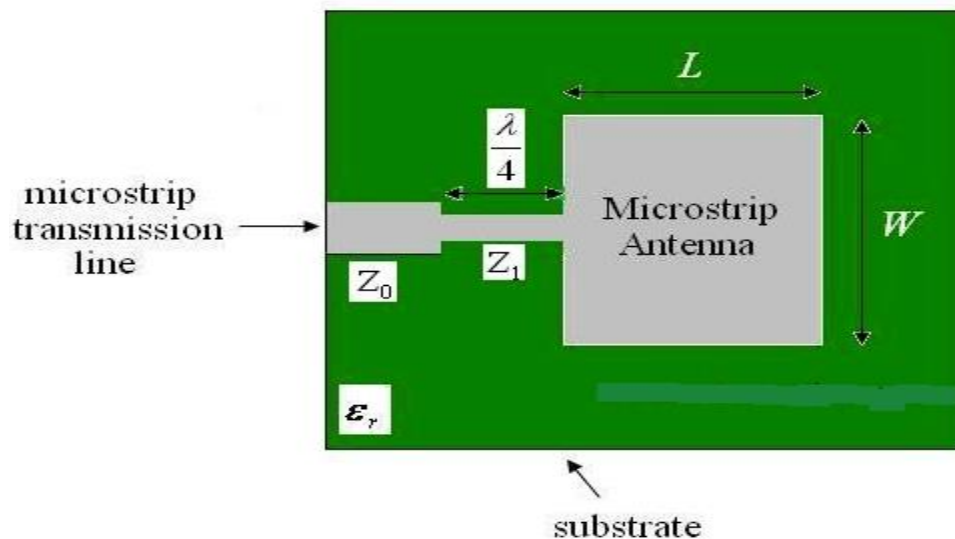


Figure 13: Patch antenna with a quarter-wavelength matching section

The goal is to match the input impedance ( $Z_{in}$ ) to the transmission line ( $Z_0$ ). If the impedance of the antenna is  $Z_A$ , then the input impedance viewed from the beginning of the quarter-wavelength line becomes

$$Z_{in} = Z_0 = \frac{Z_1^2}{Z_A}$$

This input impedance  $Z_{in}$  can be altered by selection of the  $Z_1$ , so that  $Z_{in}=Z_0$  and the antenna is impedance matched. The parameter  $Z_1$  can be altered by changing the width of the quarter-wavelength strip. The wider the strip is, the lower the characteristic impedance ( $Z_0$ ) is for that section of line.

### 1.3.3 Coaxial Cable or Probe Feed

Microstrip antennas can also be fed from underneath via a probe as shown in Figure 3. The outer conductor of the coaxial cable is connected to the ground plane, and the center conductor is extended up to the patch antenna.

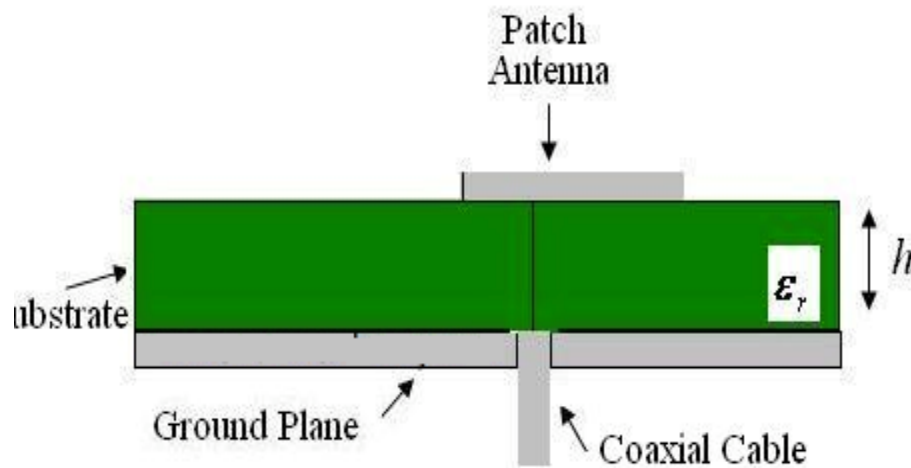


Figure 14: Coaxial cable feed of patch antenna

The position of the feed can be altered as before (in the same way as the inset feed, above) to control the input impedance.

The coaxial feed introduces an inductance into the feed that may need to be taken into account if the height  $h$  gets large (an appreciable fraction of a wavelength). In addition, the probe will also radiate, which can lead to radiation in undesirable directions.

#### 1.3.4 Coupled (Indirect) Feeds

The feeds above can be altered such that they do not directly touch the antenna. For instance, the probe feed in Figure 3 can be trimmed such that it does not extend all the way up to the antenna. The inset feed can also be stopped just before the patch antenna, as shown in Figure 4.

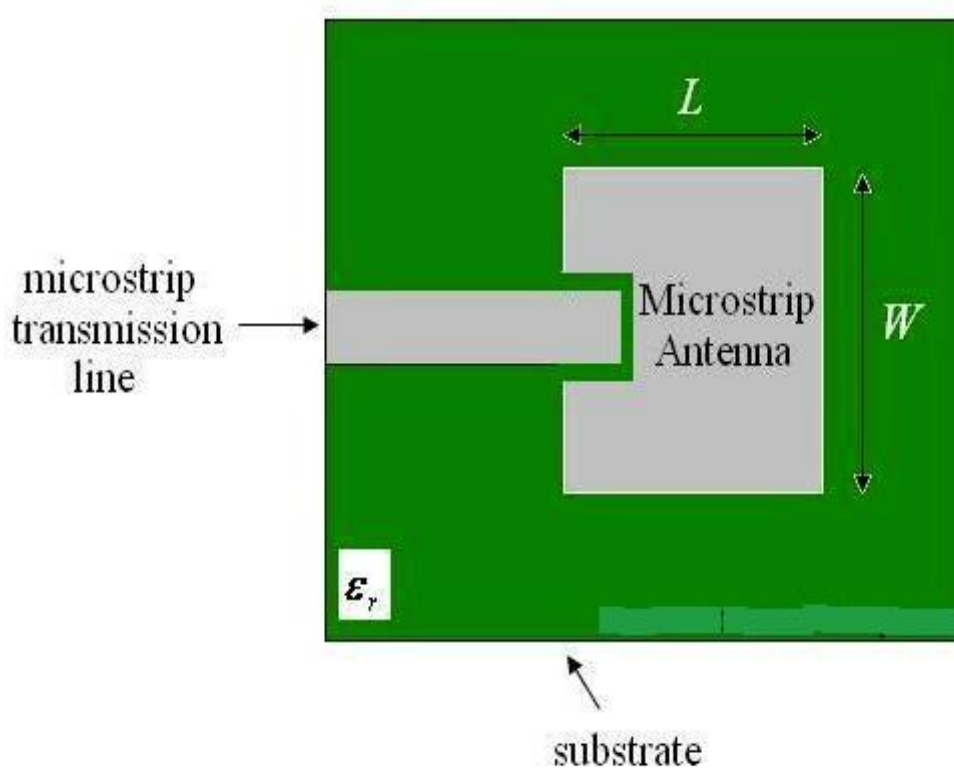


Figure 15: Coupled (indirect) inset feed.

The advantage of the coupled feed is that it adds an extra degree of freedom to the design. The gap introduces a capacitance into the feed that can cancel out the inductance added by the probe feed.

### 1.3.5 Aperture Feeds

Another method of feeding microstrip antennas is the aperture feed. In this technique, the feed circuitry (transmission line) is shielded from the antenna by a conducting plane with a hole (aperture) to transmit energy to the antenna, as shown in Figure 5.

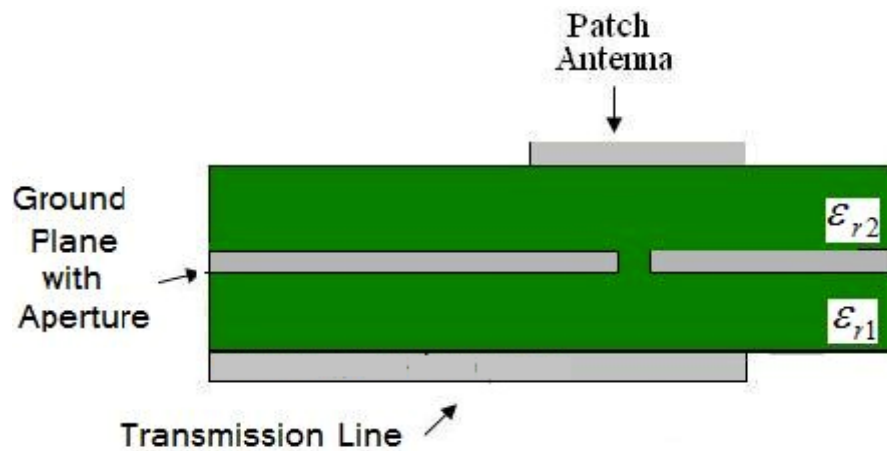


Figure 16: Aperture coupled feed.

The upper substrate can be made with a lower permittivity to produce loosely bound fringing fields, yielding better radiation. The lower substrate can be independently made with a high value of permittivity for tightly coupled fields that don't produce spurious radiation. The disadvantage of this method is increased difficulty in fabrication.

### 1.4 Antenna dimension calculation

Step 1: Calculation of the Width (W):

$$W = \frac{c}{2f_0 \sqrt{\frac{(\epsilon_r + 1)}{2}}}$$

$C = 3 \times 10^8$  m/s

$f_0 =$

$\epsilon_r =$

Using the above formula

W= 9.12871mm but we are taking W=8 by checking different values to get good results

Step 2: Calculation of the Effective Dielectric Constant. This is based on the height, dielectric constant of the dielectric and the calculated width of the patch antenna.

$$\epsilon_{eff} = \frac{\epsilon_r + 1}{2} + \frac{\epsilon_r - 1}{2} \left[ 1 + 12 \frac{h}{W} \right]^{-\frac{1}{2}}$$

=1.922

Step 3: Calculation of the Effective length

$$L_{eff} = \frac{c}{2f_0\sqrt{\epsilon_{eff}}}$$

Step 4: Calculation of the length extension  $\Delta L$

$$\Delta L = 0.412h \frac{(\epsilon_{eff} + 0.3) \left( \frac{W}{h} + 0.264 \right)}{(\epsilon_{eff} - 0.258) \left( \frac{W}{h} + 0.8 \right)}$$

=0.081 cm

Step 5: Calculation of actual length of the patch

$$L = L_{eff} - 2\Delta L$$

*L= 6.54695 but we are taking L=9 by checking various values to get good results*

**Where the following parameters are used**

f<sub>0</sub> = Resonance Frequency

W = Width of the Patch

L = Length of the Patch

h = thickness

ε<sub>r</sub> =relative Permittivity of the dielectric substrate

c = Speed of light: 3 x 10<sup>8</sup>

## 1.5 5G Technology

5G is the term used to describe the next-generation of mobile networks beyond LTE mobile networks.

The International Telecommunications Union (ITU) has released several reports on the standards for the 5G network that it refers to as the International Mobile Telecommunications (IMT)-2020 network [1].

The 3GPP is a mobile industry standards body that created its own standards for 5G New Radio specifications, published in December 2017. Both mobile operators and vendors participate in the 3GPP specification process[24].



**Figure 17: 5G standardization roadmap for 3GPP and ITU Source**

According to ITU guidelines, 5G network speeds should have a peak data rate of 20 Gb/s for the downlink and 10 Gb/s for the uplink. Latency in a 5G network could get as low as 4 milliseconds in a mobile scenario and can be as low as 1 millisecond in Ultra Reliable Low Latency Communication scenarios. Not only will people be connected to each other but so will machines, automobiles, city infrastructure, public safety and more.

5G networks are also designed to have always-on capabilities and aim to be energy efficient by minimizing how much power a modem uses based on the amount of traffic going through it.

5G ( 5th generation mobile networks or 5th generation wireless systems ) is a name used in some research papers and projects to denote the next major phase of mobile telecommunications standards beyond the upcoming 4G standards (expected to be finalized between approximately

2011 and 2013).

Currently, 5G is not a term officially used for any particular specification or in any official document yet made public by telecommunication companies or standardization bodies such as 3GPP, WiMAX Forum or ITU-R. New 3GPP standard releases beyond 4G and LTE Advanced are in progress, but not considered as new mobile generations. The implementation of standards under a 5G umbrella would likely be around the year of 2020.

5G Technology stands for 5th Generation Mobile technology. 5G technology has changed the means to use cell phones within very high bandwidth. User never experienced ever before such a high value technology. Nowadays mobile users have much awareness of the cell phone (mobile) technology. The 5G technologies include all type of advanced features which makes 5G technology most powerful and in huge demand in near future

5G Technologies have an extraordinary capability to support Software and Consultancy. The Router and switch technology used in 5G network providing high connectivity. The 5G technology distributes internet access to nodes within the building and can be deployed with union of wired or wireless network connections. The current trend of 5G technology has a glowing future.

The 5G terminals will have software defined radios and modulation schemes as well as new error-control schemes that can be downloaded from the Internet. The development is seen towards the user terminals as a focus of the 5G mobile networks. The terminals will have access to different wireless technologies at the same time and the terminal should be able to combine different flows from different technologies. The vertical handovers should be avoided, because they are not feasible in a case when there are many technologies and many operators and service providers. In 5G, each network will be responsible for handling user-mobility, while the terminal will make the final choice among different wireless/mobile access network providers for a given service. Such choice will be based on open intelligent middleware in the mobile phone[1,3,5,24].

### **Network Layer:**

The network layer will be IP (Internet Protocol), because there is no competition today on this level. The IPv4 (version 4) is worldwide spread and it has several problems such as limited address space and has no real possibility for QoS support per flow. These issues are solved in IPv6, but traded with significantly bigger packet header. Then, mobility still remains a problem.

There is Mobile IP standard on one side as well as many micro-mobility solutions (e.g., Cellular IP, HAWAII etc.). All mobile networks will use Mobile IP in 5G, and each mobile terminal will be FA (Foreign Agent), keeping the CoA (Care of Address) mapping between its fixed IPv6 address and CoA address for the current wireless network. However, a mobile can be attached to several mobile or wireless networks at the same time. In such case, it will maintain different IP addresses for each of the radio interfaces, while each of these IP addresses will be CoA address for the FA placed in the mobile Phone. The fixed IPv6 will be implemented in the mobile phone by 5G phone manufactures.

The 5G mobile phone shall maintain virtual multi-wireless network environment. For this purpose there should be separation of network layer into two sub-layers in 5G mobiles (Fig. ) i.e.: Lower network layer (for each interface) and Upper network layer (for the mobile terminal). This is due to the initial design of the Internet, where all the routing is based on IP addresses which should be different in each IP network worldwide. The middleware between the Upper and Lower network layers (Fig. 3) shall maintain address translation from Upper network address (IPv6) to different Lower network IP addresses (IPv4 or IPv6), and vice versa.

#### Features

- ✓ 5G technology offer high resolution for crazy cell phone user and bi- directional large bandwidth shaping.
- ✓ The advanced billing interfaces of 5G technology makes it more attractive and effective.
- ✓ 5G technology also providing subscriber supervision tools for fast action.
- ✓ The high quality services of 5G technology based on Policy to avoid error.
- ✓ 5G technology is providing large broadcasting of data in Gigabit which supporting almost 65,000 connections.
- ✓ 5G technology offer transporter class gateway with unparalleled consistency.
- ✓ The traffic statistics by 5G technology makes it more accurate.
- ✓ Through remote management offered by 5G technology a user can get better and fast solution.
- ✓ The remote diagnostics also a great feature of 5G technology.



- ✓ The 5G technology is providing up to 25 Mbps connectivity speed.
- ✓ The 5G technology also support virtual private network.
- ✓ The new 5G technology will take all delivery service out of business prospect
- ✓ The uploading and downloading speed of 5G technology touching the peak.

## 1.6 ANSYS HFSS

ANSYS HFSS is 3D electromagnetic (EM) simulation software for designing and simulating high-frequency electronic products such as antennas, antenna arrays, RF or microwave components, high-speed interconnects, filters, connectors, IC packages and printed circuit boards. Engineers worldwide use ANSYS HFSS to design high-frequency, high-speed electronics found in communications systems, radar systems, advanced driver assistance systems (ADAS), satellites, internet-of-things (IoT) products and other high-speed RF and digital devices.

HFSS (High Frequency Structure Simulator) employs versatile solvers and an intuitive GUI to give you unparalleled performance plus deep insight into all your 3D EM problems. Through integration with ANSYS thermal, structural and fluid dynamics tools, HFSS provides a powerful and complete multiphysics analysis of electronic products, ensuring their thermal and structural reliability. HFSS is synonymous with gold standard accuracy and reliability for tackling 3D EM challenges by virtue of its automatic adaptive meshing technique and sophisticated solvers, which can be accelerated through high performance computing (HPC) technology.

The ANSYS HFSS simulation suite consists of a comprehensive set of solvers to address diverse electromagnetic problems ranging in detail and scale from passive IC components to extremely large-scale EM analyses such as automotive radar scenes for ADAS systems. Its reliable automatic adaptive mesh refinement lets you focus on the design instead of spending time determining and creating the best mesh. This automation and guaranteed accuracy differentiates HFSS from all other EM simulators, which require manual user control and multiple solutions to ensure that the generated mesh is suitable and accurate. With ANSYS HFSS, the physics defines the mesh rather than the mesh defining the physics.

ANSYS HFSS is the premier EM tool for R&D and virtual design prototyping. It reduces design cycle time and boosts your product's reliability and performance. Beat the competition and capture your market with ANSYS HFSS.

## CHAPTER 2

### 2. LITERATURE SURVEY

**Table 1: Literature Survey**

Sr no	Title	Year	Design	Feed line	Substrate Width	Substrate Length	Thickness	Frequency	S11 (dB)	Dielectric Constant	Gain
1	Multiband Low profile printed monopole antenna for Future 5G Wireless Application With DGS	2017	Patch	Inset feed	58.5mm	10mm	1.4mm	28GHz	-23	RT5580 (2.2)	
2	Design of a Dual-Band printed slot Antenna with Utilizing a Band Rejection element for 5G wireless Applications	2016	Patch	Inset feed	5mm	5mm	0.127mm	28/38GHz	-46	RT5580 (2.2)	3.6-4.4 dB
3	A 9-shaped Antenna for 5G Applications	2017	9 shape patch	Inset feed	30mm	38mm	1.6mm	24.5 – 27.5 GHz		FR4 (4.4)	(1.94 -10 )dB
4	A Wideband mm-Wave Printed Dipole Antenna for 5G Applications	2018	Array	Coaxial feed	5.85mm	7.35mm		24 GHz, 25 GHz, 28 GHz, 32 GHz, 38 GHz 40GHz	<- 10	RT5880 (2.2)	5.34 dB
5	A Compact Elliptical Microstrip Patch Antenna for Future 5G Mobile Wireless Communication	2017	Patch	Inset feed	5mm	5mm	1.6mm	28	-45	FR4 (4.4)	
6	Multiband Antennas Design Techniques for 5G Networks: Present and	2018		-----	-----	-----	-----	-----	-----	-----	-----

	Future Research Directions										
7	Design of Microstrip Patch Antenna for 5g Applications	2017	Patch	Feed line	----	-----	0.5mm	28.3 GHz	- 30.7774	RT 5880	2.6 dB
8	Wide-band Circular Antenna for 5G Applications	2018	Patch	Inset feed	50mm	50mm	-----	24.5-27.5 GHz, 31.8-33.4 GHz and 40.5-43.5 GHz.	<- 10	RT 5880	
9	A Novel Planar Slot Antenna Structure for 5G Mobile Networks Applications	2017	Patch	Inset feed	4mm	26mm	1.6mm	6.37 GHz and 14.06 GHz	< - 10	Feko simulator and ADS (4.4)	11.13 dB
10	A Microstrip Patch Antenna Design at 28GHz for 5G Mobile Phone Applications	2018	Patch	Inset feed	4.5mm	5.5mm	0.4mm	28GHz	< - 10	FR4 (4.4)	2.875 dB
11	A compact printed RFID reader dipole array antenna for 5G- IOT applications	2018	RFID Reader	Coaxial feed	2mm	4mm	0.127mm	64Hz	<- 10	FR(2.55)	20dB
12	Characteristics of beam faced array antenna for 5G applications	2017	-	-	-	-	-	38GHz	-	-	16.2dB
13	Slot antenna design for 5G Mobile networks	2017	slot	Coaxial feed	4mm	26mm	4.4mm	8.69GHz	-	Feko	6.14dB
14	Wideband high gain antenna sub array for 5G application	2017	High gain	Inst feed	2mm	4mm	0.125mm	28GHz	-	-	12dB

## CHAPTER 3

### 3. EXPERIMENT WORK

#### 3.1 Flow Diagram

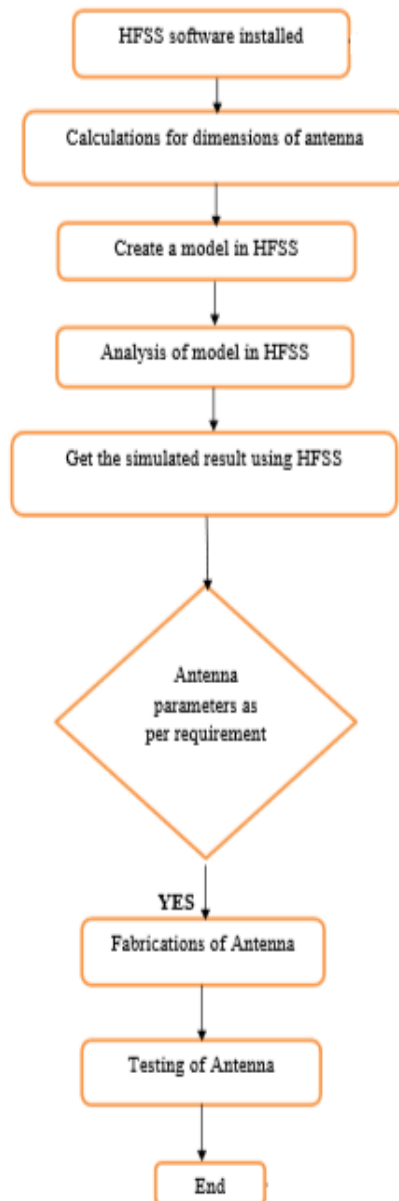
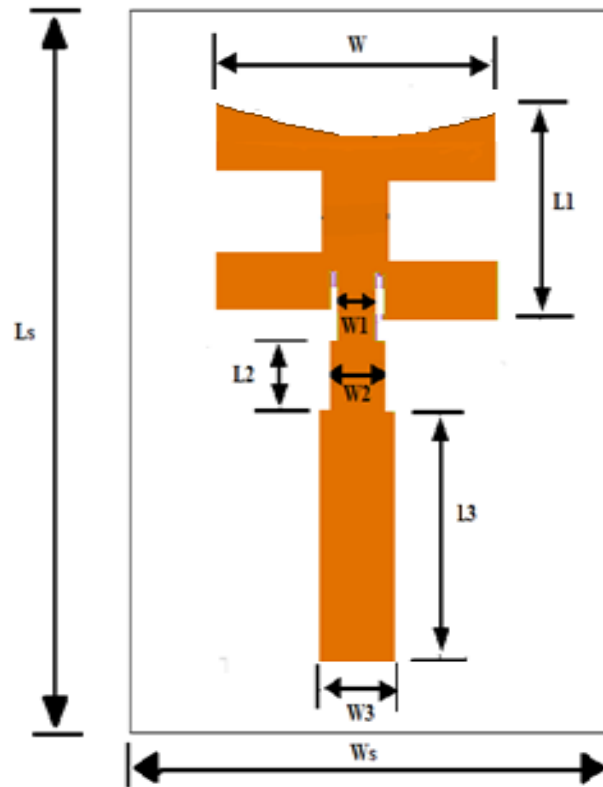


Figure 18: Flow diagram for design the antenna

### 3.1 Antenna Design and Geometry

The top view of the proposed antenna is shown in Fig.1. The radiating element is a monopole, having concave-rectangular shape with the edge having a well-defined curvature. The monopole is inset fed with a microstrip line that has a step transition to obtain optimum matching.



**Figure 19: Geometry of the first proposed antenna**

The substrate used for the considered design is FR4 epoxy having a dielectric constant of  $\epsilon_r = 4.4$ . The thickness of the substrate is 1.4mm whereas the width and the length are given as 8x9 mm<sup>2</sup> respectively. The dimensions of the monopole antenna are reflected in Table 2.

Table 2 Dimensions of proposed antenna in mm

PARAMETER	VALUE	PARAMETER	VALUE
L1	3.1	W1	1
L2	2.8	W2	2
L3	4.7	W3	2.2
Ls	9	Ws	8
W	7.6		

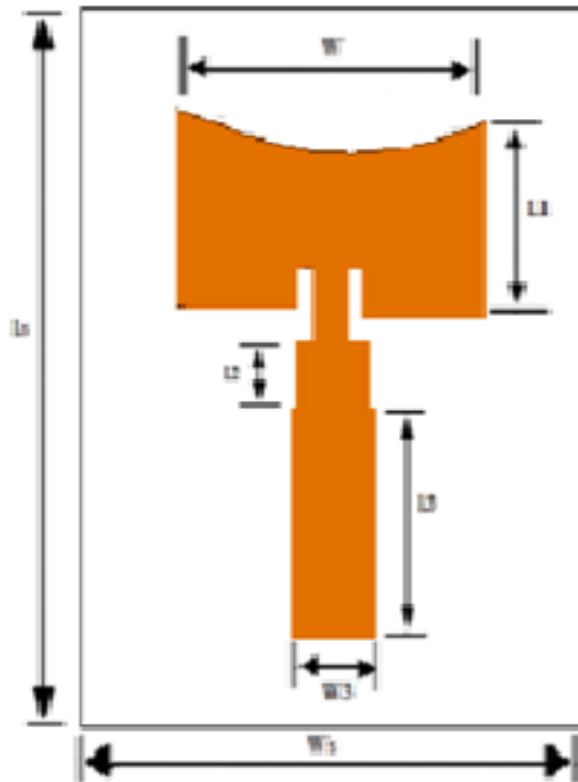
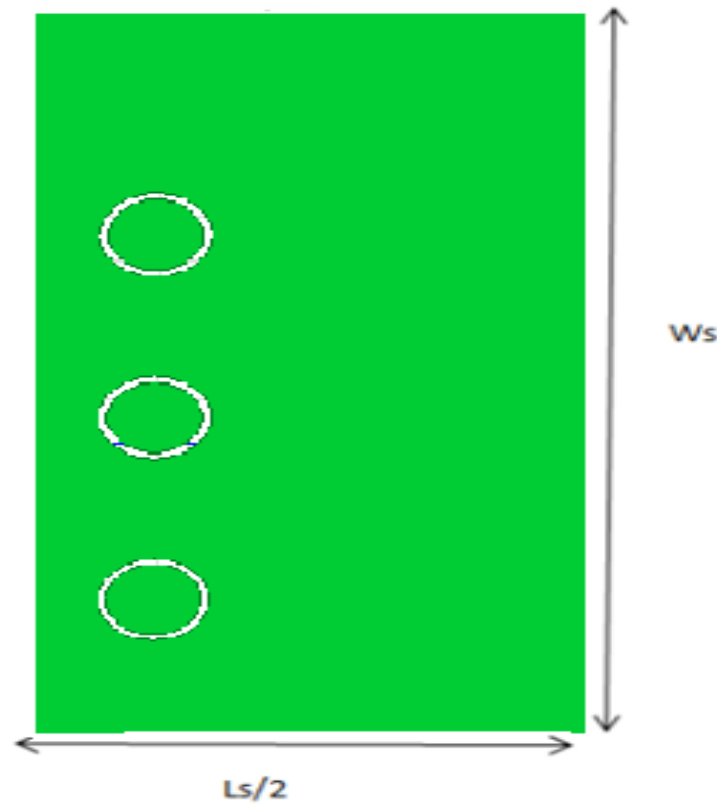


Figure 20: Geometry of the second proposed antenna

**Table 3: dimensions of the second antenna**

PARAMETER	VALUE(mm)	PARAMETER	VALUE(mm)
PL	3.1	W1	2.2
PW	7.6	W2	1
L1	4.7	W3	0.6
L2	1.2	Ws	8
L3	1	Ls	9

The ground plane comprising of three circular slots is a defected ground structure (DGS) as shown in Fig21. The outer radii of the circular slots are 0.46mm and the inner radii are 0.39mm. The resulting antenna provides wide bandwidth coverage as compared to other antennas and is small in size with high performance results.

**Figure 21: Back view of the proposed antenna**



## CHAPTER 4

### 4. RESULTS AND DISCUSSION

The simulations of the proposed patch antenna structure were performed using HFSS software. The antenna performances were evaluated in terms of return loss, VSWR, E and H plane radiation plots and gain.

The validation of simulated results will then be performed by testing and measurement. This section explains the comparison between the different designs that were worked on and from there how the current design, emerged to be the best for the proposal.

#### 4.1 Return Loss (RL):

This parameter indicates the matching between the transmitter and antenna. If the return loss of an antenna for a specific frequency is less than -10dB, it indicates that the power fed to the antenna out of the maximum power is accepted and that the element is good at radiating.

#### 4.2 VSWR (Voltage Standing Wave Ratio)

For an efficient performance of the antenna, the VSWR tolerance is 2 practically (between one and two), along the band it operates. The VSWR plot confirmed that the proposed antenna has proper impedance matching.

#### 4.3 Antenna Gain

The gain of an antenna in the given direction is defined as the ratio of intensity in a given direction to the radiation intensity that would be obtained if the power accepted by the antenna were radiated isotopically. The gain of our design gives worthy results.

#### 4.4 Results for the proposed antenna 1

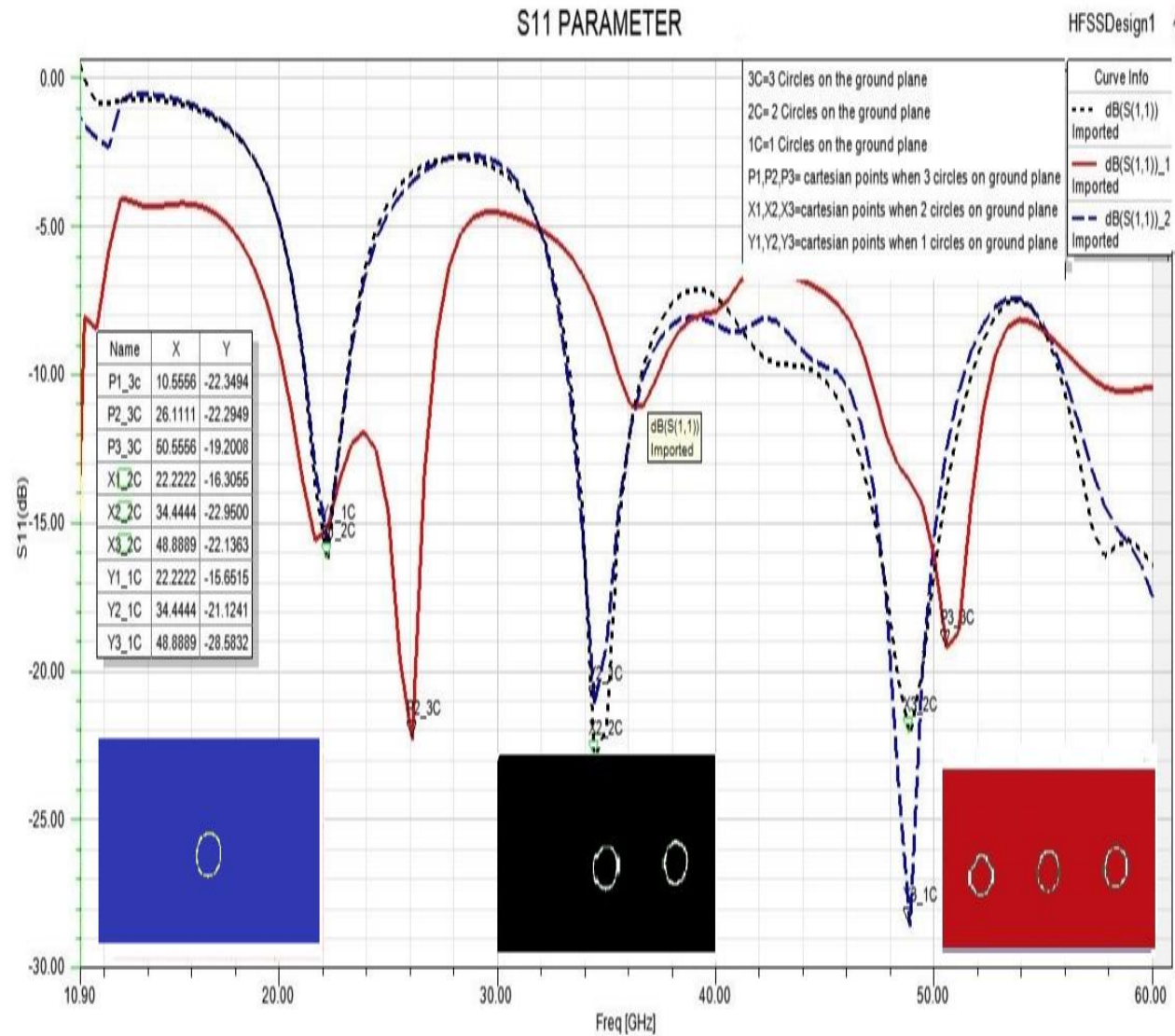


**Figure 22: Simulation results for S11 parameter for the ground plane**

As shown in fig.22, the plot for S11 parameter is generated for the ground plane having 1, 2 and 3 circular slots on it using HFSS software. It is found that the best results are obtained when there are 3 circular slot on the ground plane since the values obtained are -22.3dB, -22.29dB and -19.2dB for the respective dips at the three points. In contrast when 2 circles are considered the values obtained are -16dB, -22dB and -22dB, while for 1 circular slot on the ground plane, the values obtained are -15dB, -21dB and -28dB. Thus it is better to go for the ground plane having 3 circular slots.

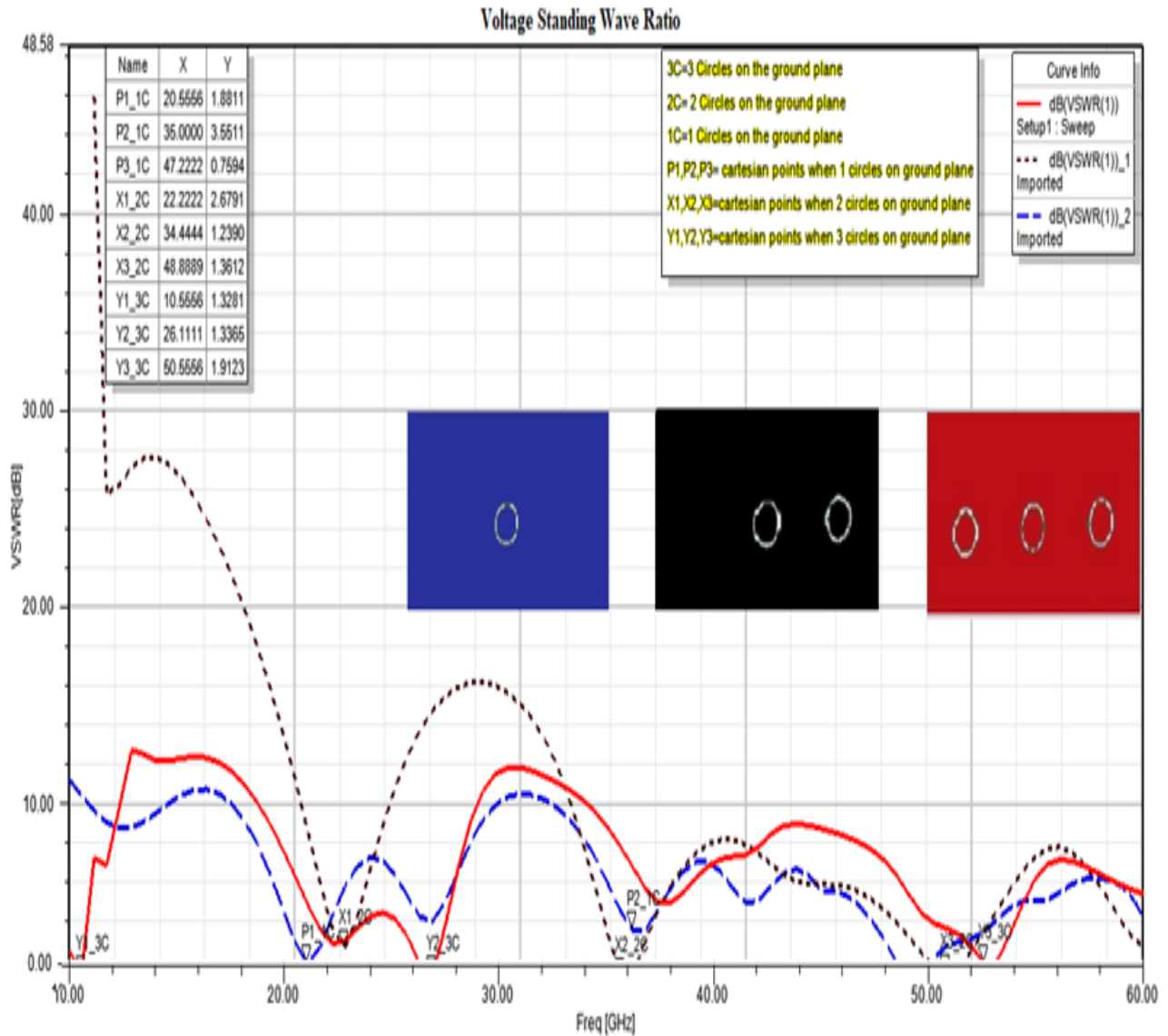


**Figure 23: Simulation Results for VSWR for the ground plane**

As shown in fig.23, the plot for VSWR is generated for the ground plane having 1 2 and 3 circular slot on it using HFSS software. It is found that the best results are obtained when there are 3 circular on the ground plane since the values obtained are 1.32, 1.33 and 1.91 for the respective dips at the three points. In contrast, when 2 circular are considered the values obtained are 2.6, 1.2 and 1.3, while for 1 circle on the ground plane, the values obtained are 1.8, 3.5 and 0.75. Thus it is better to go for the ground plane having 3 circular slot.

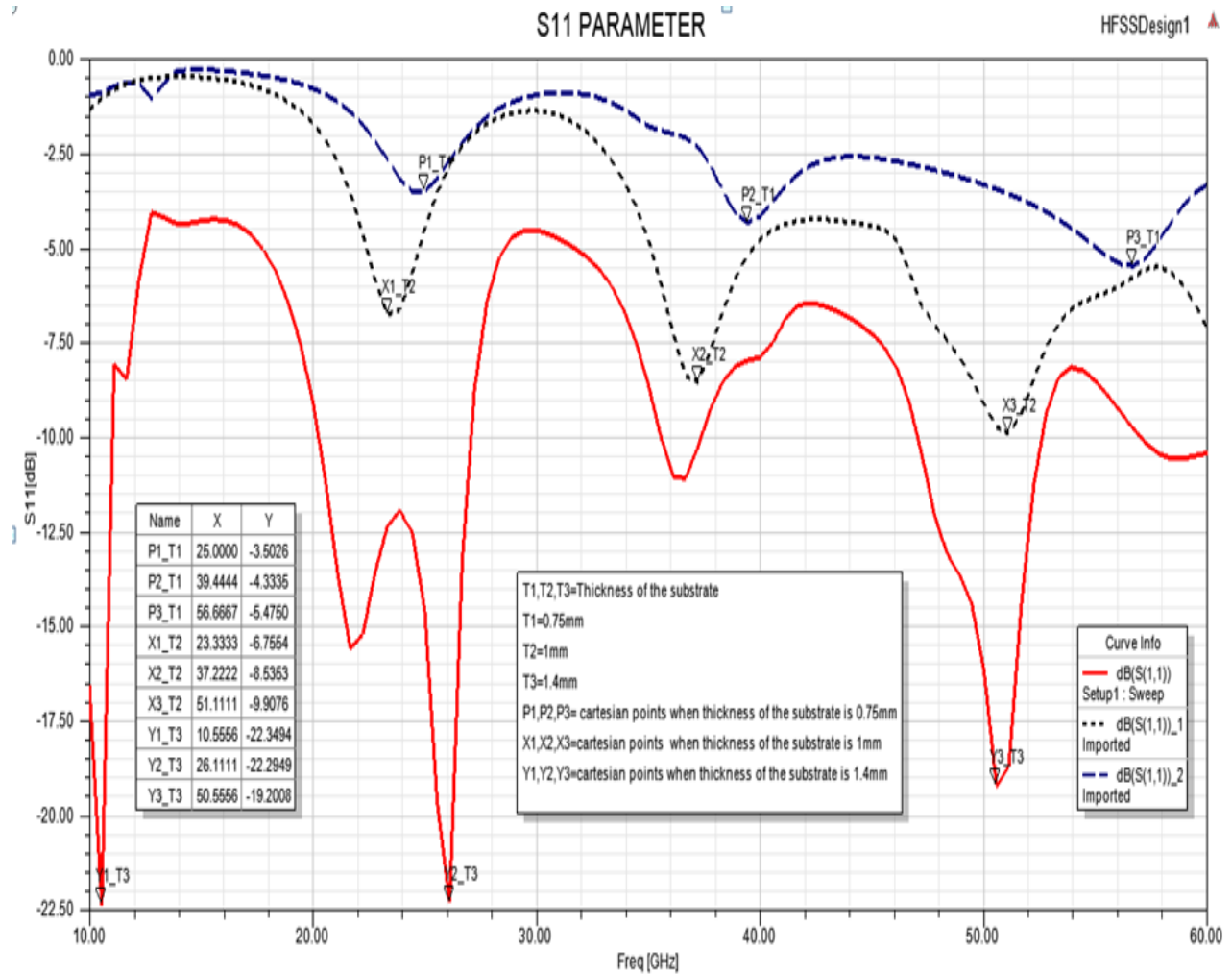


**Figure 24: Simulation Results for S11 parameter for thickness of the substrate**

As shown in fig.24, the plot for S11 parameter is generated for 3 different thicknesses of the substrate depending on the number of circular slot on the ground plane using HFSS software. It is found that the best results are obtained when there are 3 circular slots on the ground plane since the values obtained are -22.3dB, -22.29dB and -19.2dB for the respective dips at the three points. In contrast when 2 circular slots are considered the values obtained are -6dB, -8dB and -9dB, while for 1 circle on the ground plane, the values obtained are -3dB, -4dB and -5dB. Thus, ground plane having circular slots is considered.

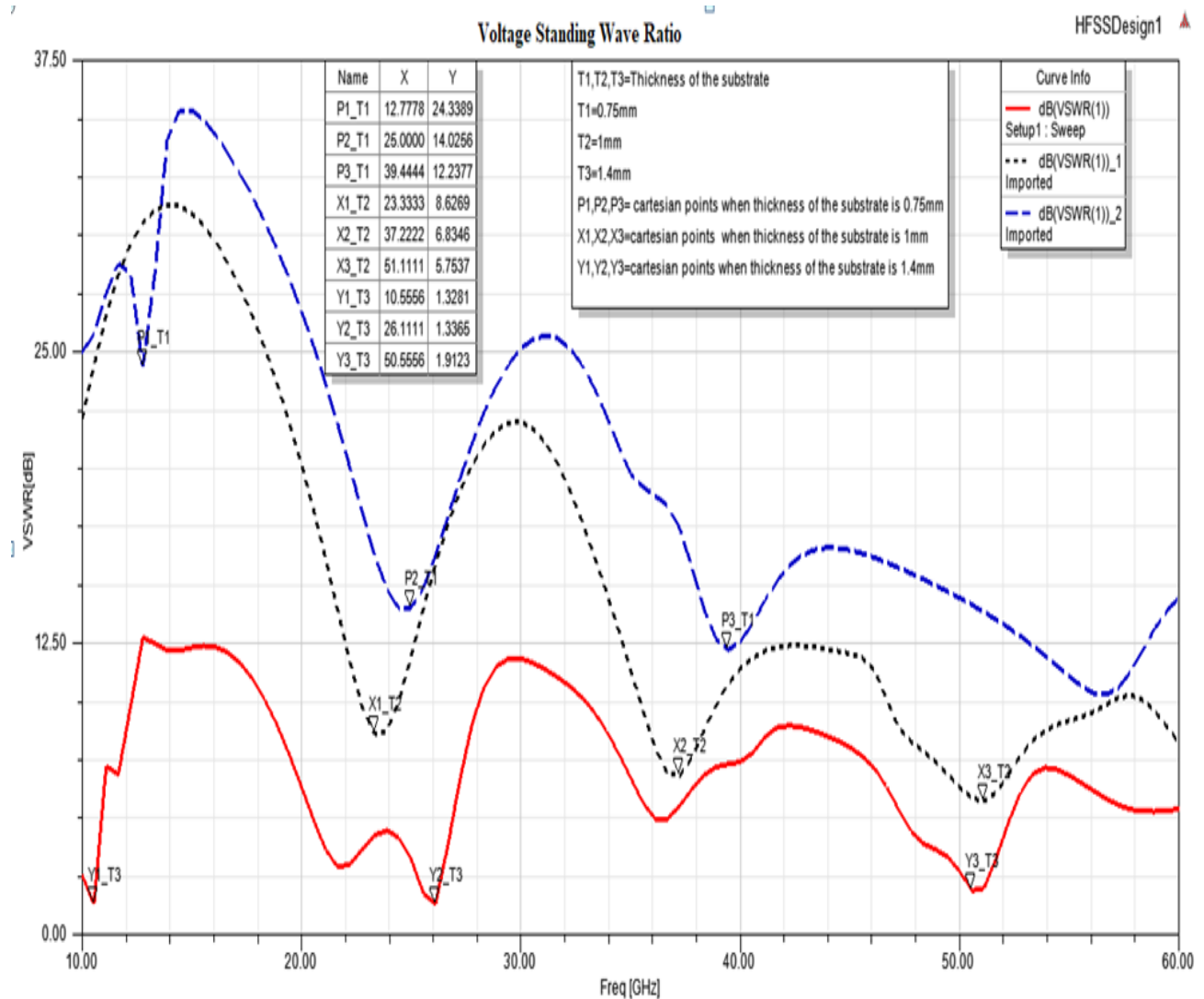


**Figure 25: Simulation Results for the VSWR for the thickness of the substrate**

As shown in fig.25, the plot for VSWR is generated for 3 different thicknesses of the substrate depending on the number of circular slots on the ground plane using HFSS software. It is found that the best results are obtained when there are 3 circular slots on the ground plane since the values of obtained are 1.3, 1.3 and 1.9 for the respective dips at the three points. In contrast when 2 circular slots are considered the values obtained are 8, 6 and 5, while for 1 circular slot on the ground plane, the values obtained are 24, 14 and 12. Thus, ground plane having 3 circular slots is considered.

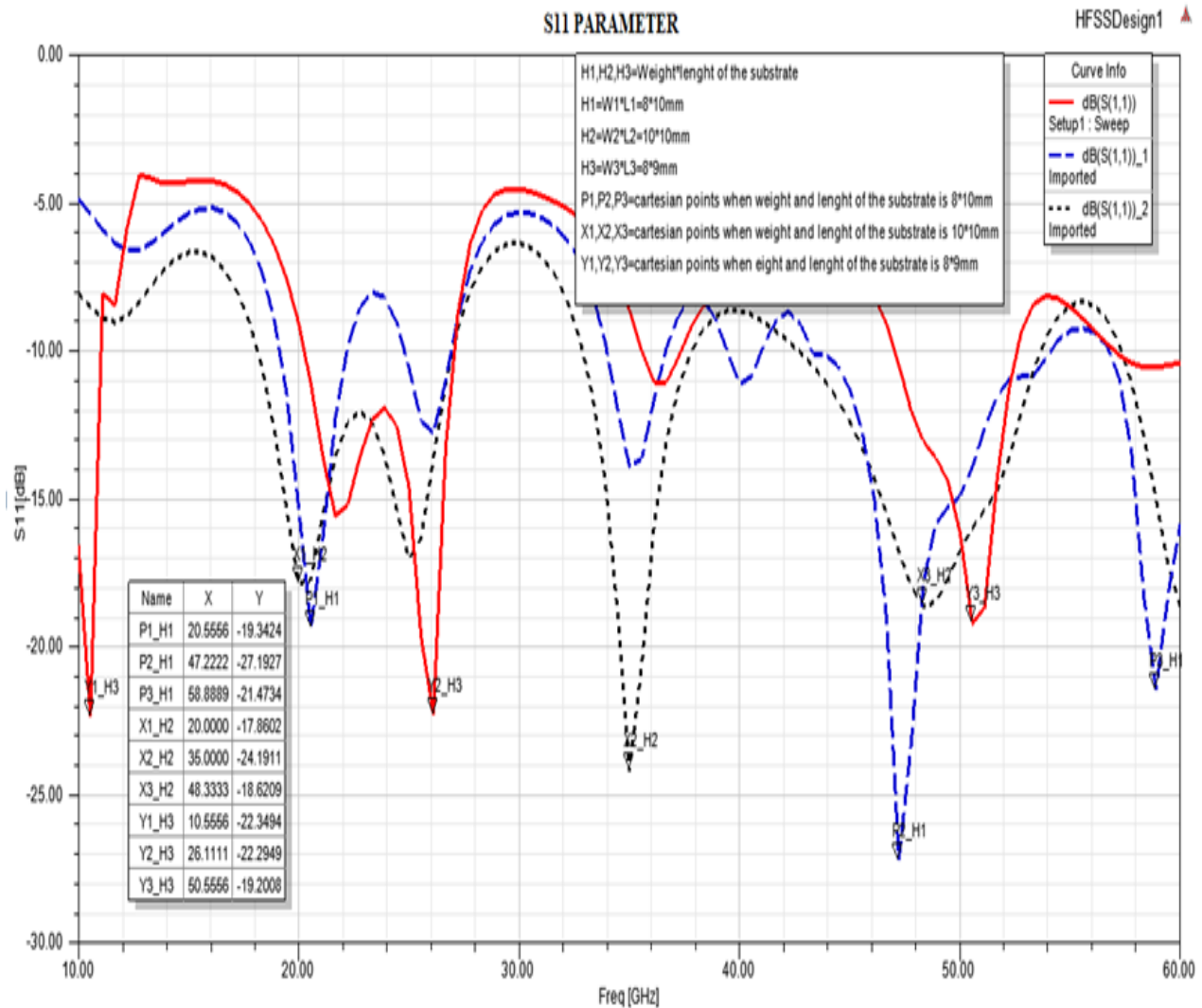


**Figure 26: Simulation Results for S11 parameter for the height of the substrate**

As shown in fig.26, the plot for S11 parameter is generated for 3 different heights of the substrate depending on the number of circles on the ground plane using HFSS software. It is found that the best results are obtained when there are 3 circles on the ground plane since the values obtained are -22.3dB, -22.29dB and -19.2dB for the respective dips at the three points. In contrast when 2 circles are considered the values obtained are -17dB, -24dB and -18dB, while for 1 circle on the ground plane, the values obtained are -19dB, -27dB and -21dB. Thus, ground plane having 3 circles is considered.

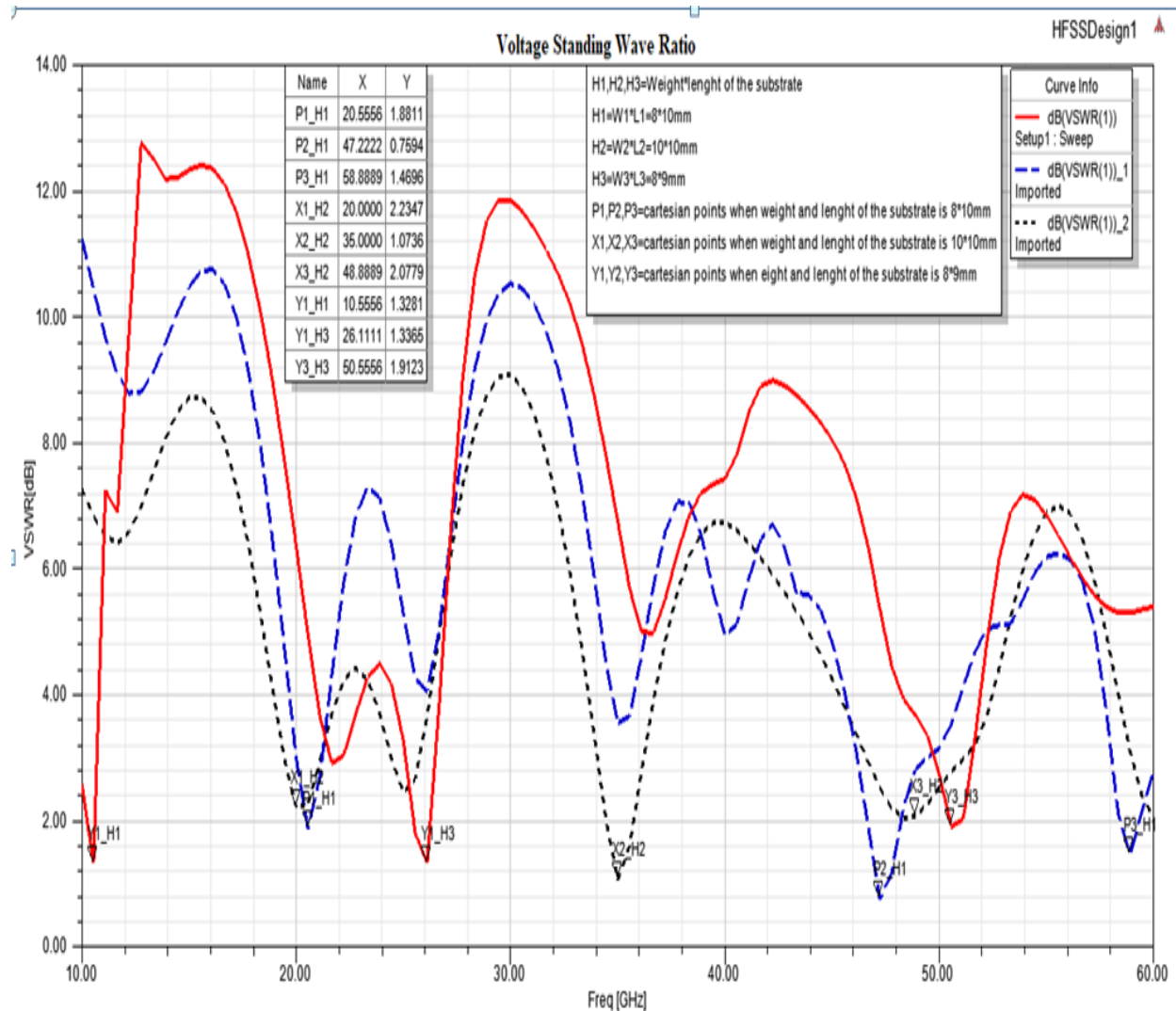


**Figure 27: Simulation Results for VSWR for the height of the substrate**

As shown in fig.27, the plot for VSWR is generated for 3 different heights of the substrate depending on the number of circles on the ground plane using HFSS software. It is found that the best results are obtained when there are 3 circles on the ground plane since the values of obtained are 1.3, 1.3 and 1.9 for the respective dips at the three points. In contrast when 2 circles are considered the values obtained are 1, 2 and 1.3, while for 1 circle on the ground plane, the values obtained are 1.8, 0.7 and 1.4. Thus, ground plane having 3 circles is consider



#### 4.4.1 Radiation patterns for different frequency bands

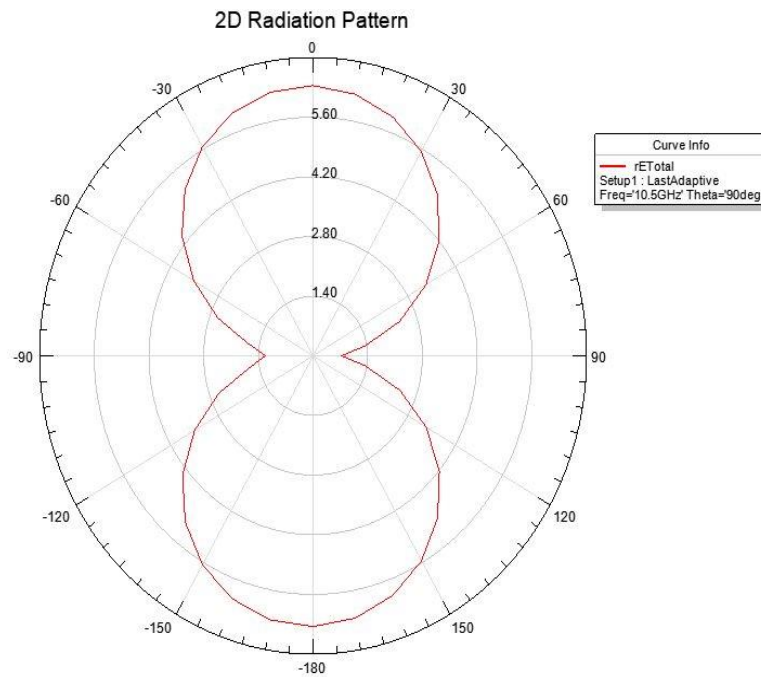


Figure 28:2D pattern for 10.5GHz band at 90 degrees

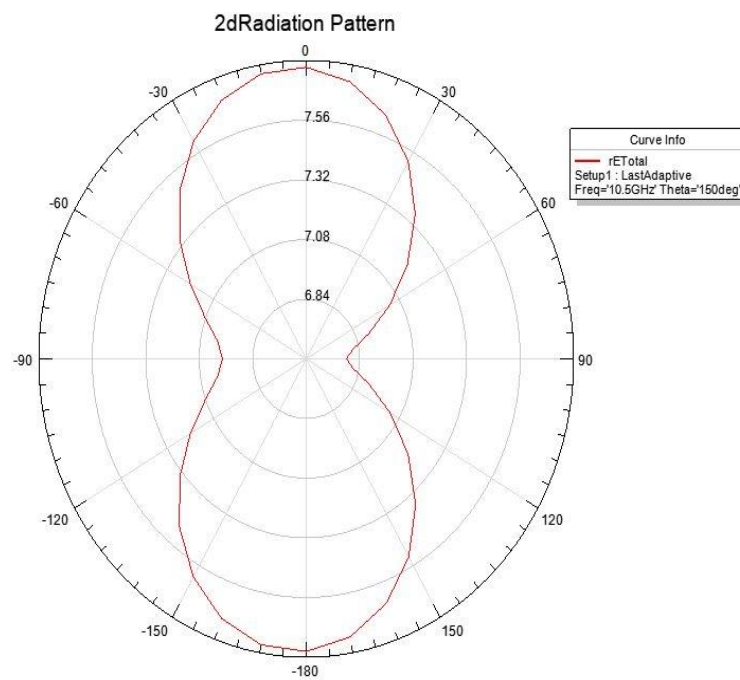
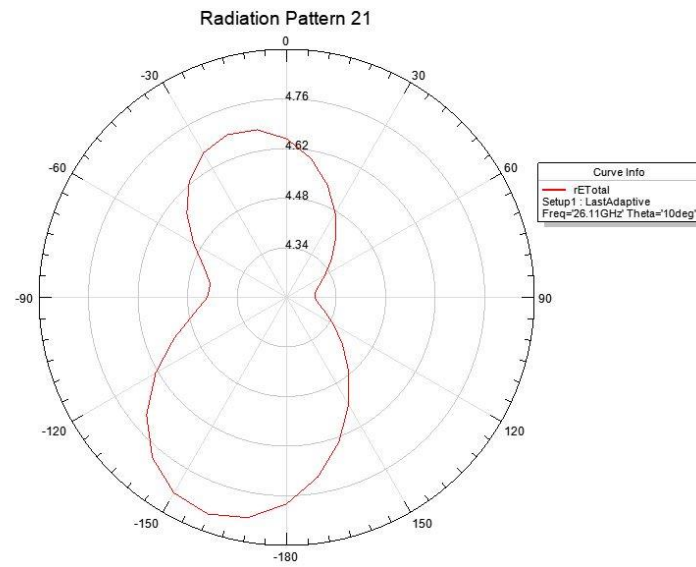
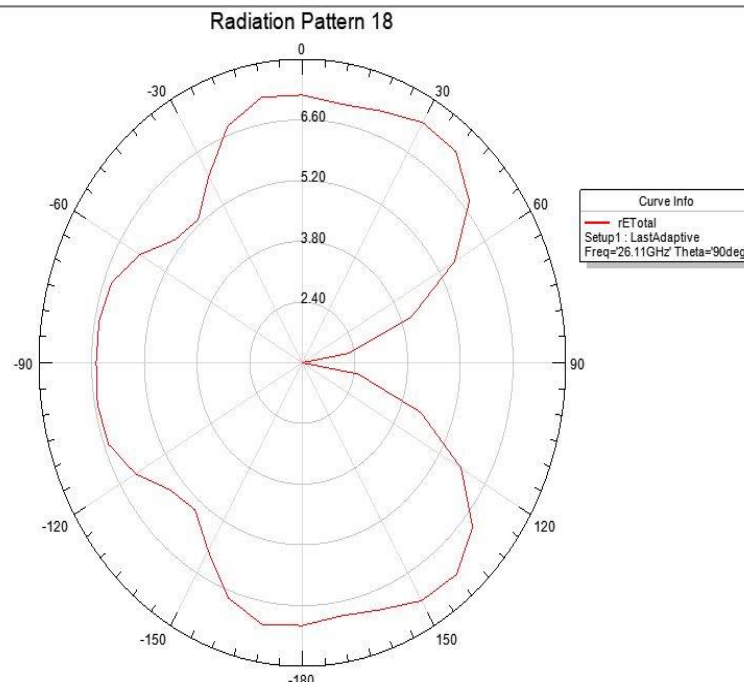


Figure 29:2D pattern for 10.5GHz band at 150 degrees





**Figure 30: 2D pattern for 26.11GHz band at 10 degrees**



**Figure 31: 2D pattern for 26.11GHz band at 90 degrees**

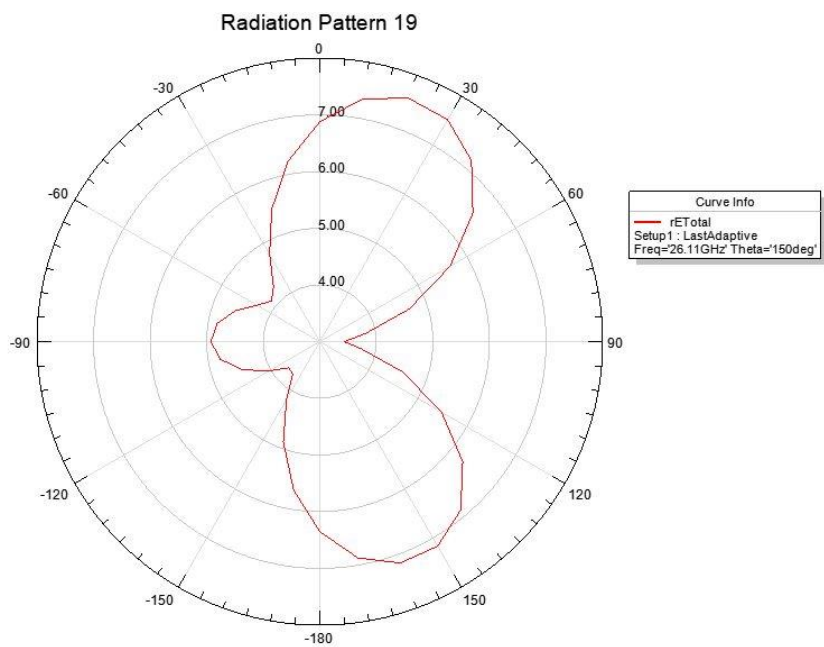


Figure 32: 2D pattern for 26.11GHz band at 150 degrees

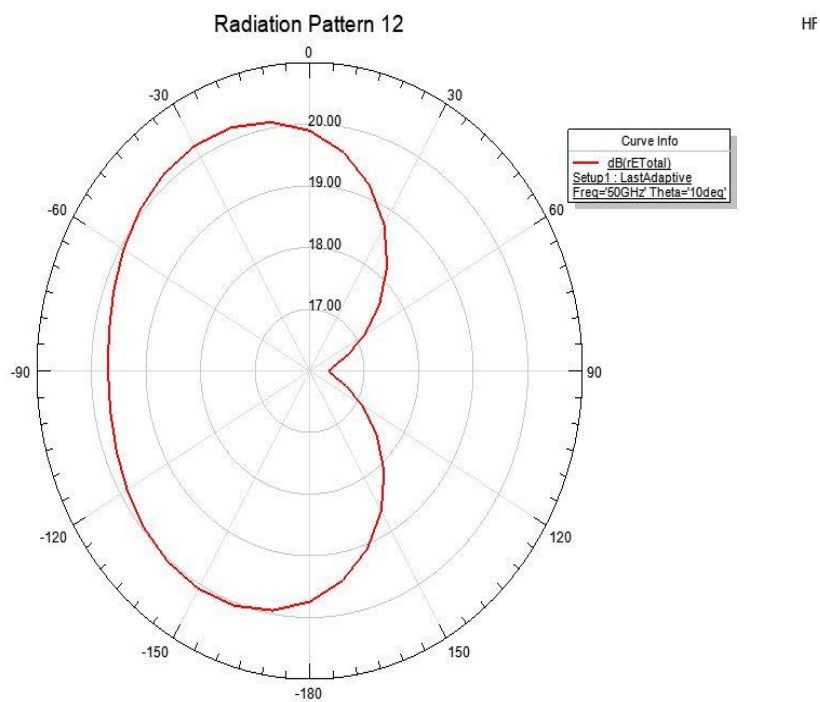


Figure 33: 2D pattern for 50GHz band at 10 degrees

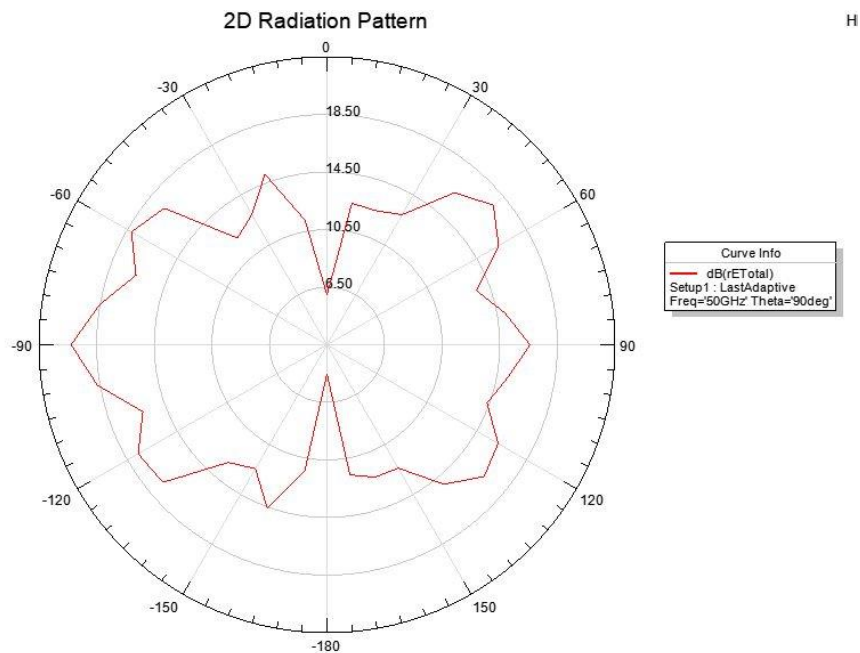


Figure 34: 2D pattern for 50GHz band at 90 degrees

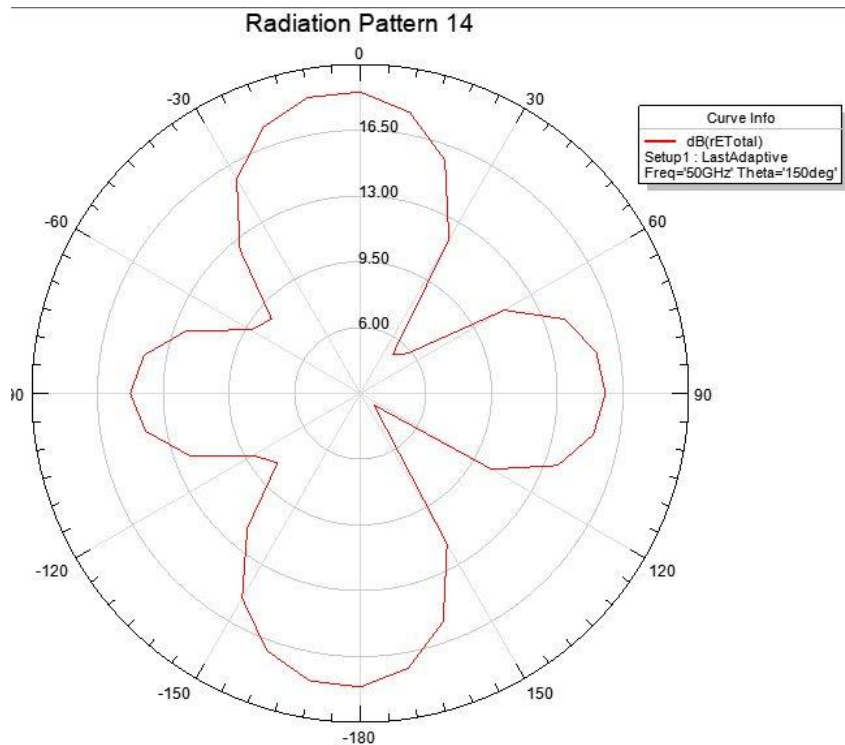


Figure 35: 2D pattern for 50GHz band at 150 degrees

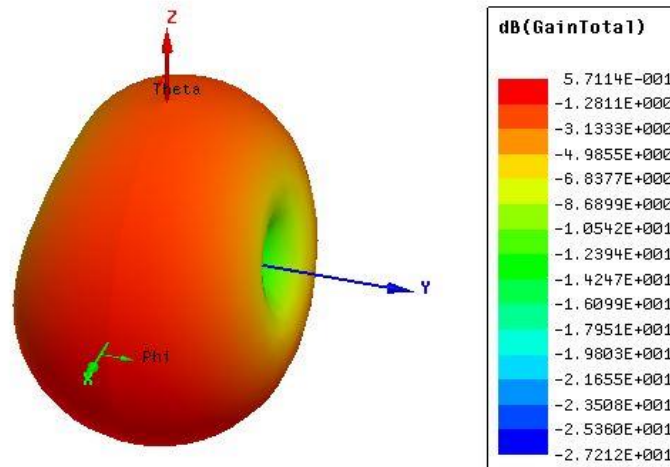


Figure 36: 3D pattern for 10.5GHz band

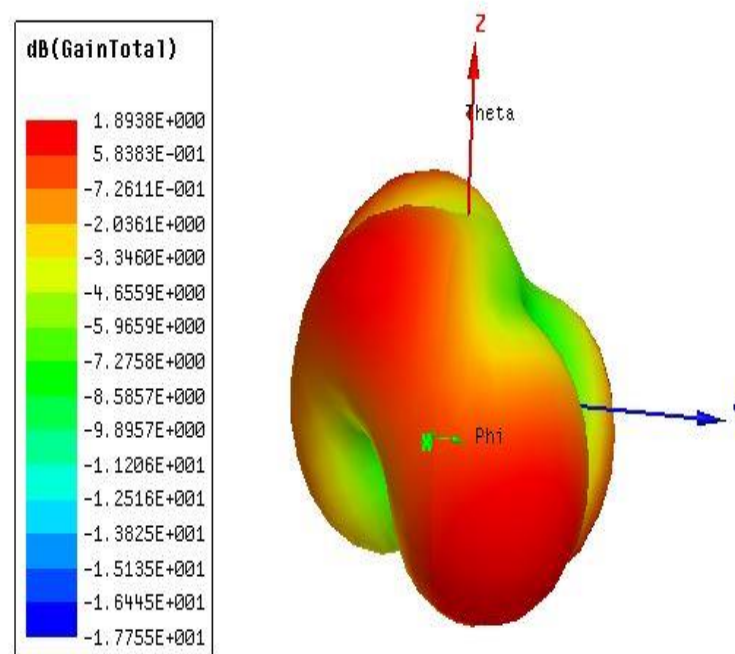


Figure 37: 3D pattern for 26.11GHz band

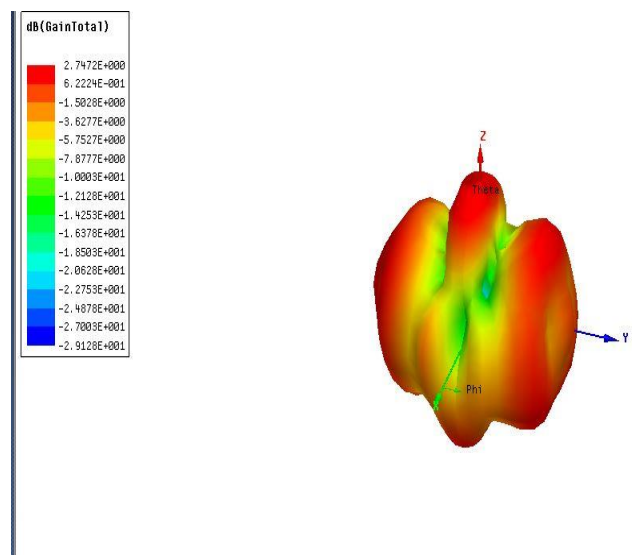


Figure 38: 3D pattern for 50 GHz band

4.5 Results for proposed antenna 2

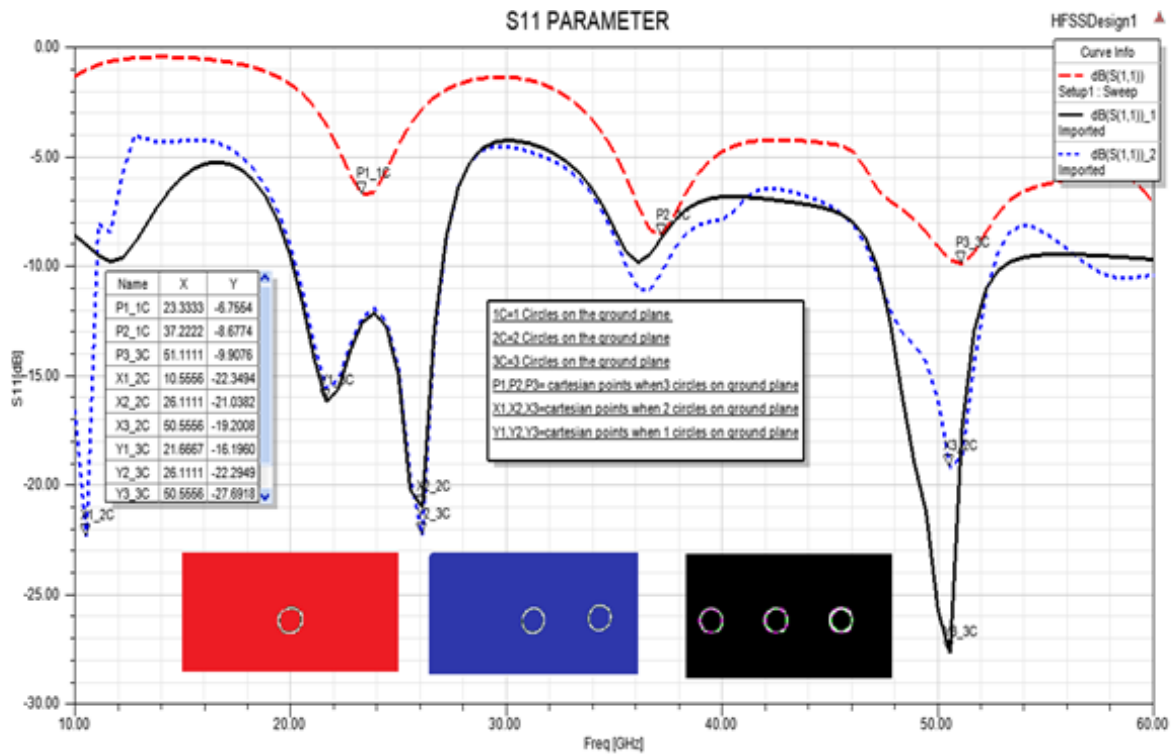
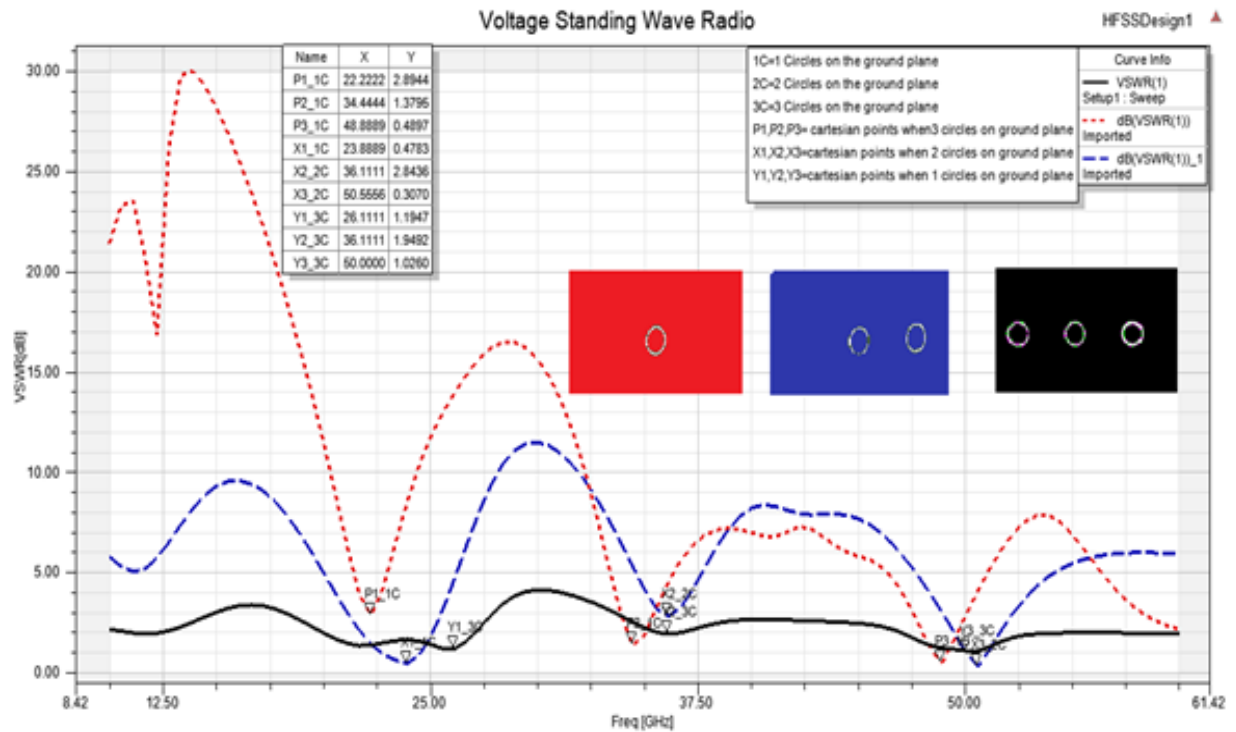


Figure 39:: Simulation results for S11 parameter for the ground plane

As shown in fig.39, the plot for S11 parameter is generated for the ground plane having 1, 2 and 3 circular slots on it using HFSS software. It is found that the best results are obtained when there are 3 circular slots on the ground plane since the values obtained are -15.19dB,-22.2dB,-27.6dB for the respective dips at the three points. In contrast when 2 circles are considered the values obtained are, while for 1 circle on the ground plane, the values obtained are. Thus it is better to go for the ground plane having 3 circular slots .



**Figure 40: Simulation Results for VSWR**

As we know that the ideal value of VSWR is 1, but practically, it is from 1 to 2. In our design for all three bands we are getting the best value of VSWR, which is nearly equal to the ideal values. The fig.40, the plot for VSWR is generated for the ground plane having 1, 2 and 3 circular slots on it using HFSS software. It is found that the best results are obtained when there are 3 circular slots on the ground plane since the values obtained are 1.1, 1.9 and 1.1 for the respective dips at the three points. In contrast, when 1 and 2 circular slots are considered the values obtained are not the expected values, Thus it is better to go for the ground plane having 3 circles.

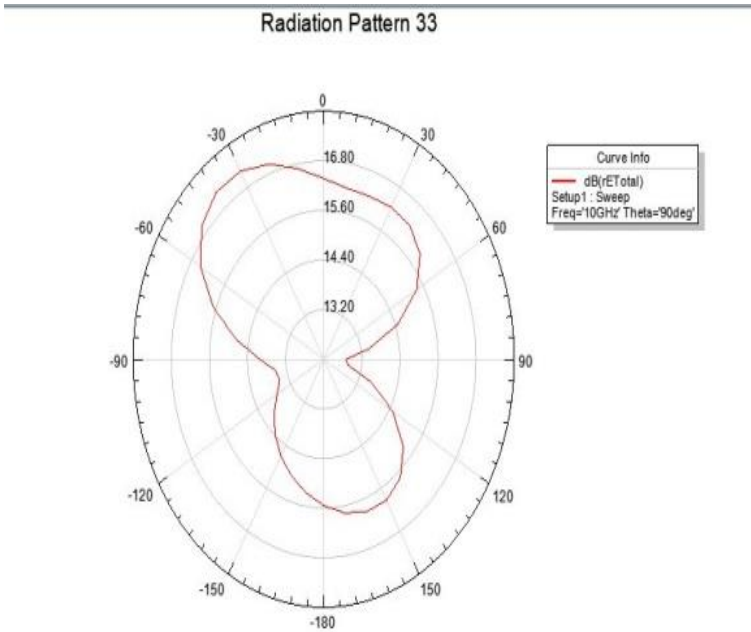


Figure 41: 2D radiation pattern

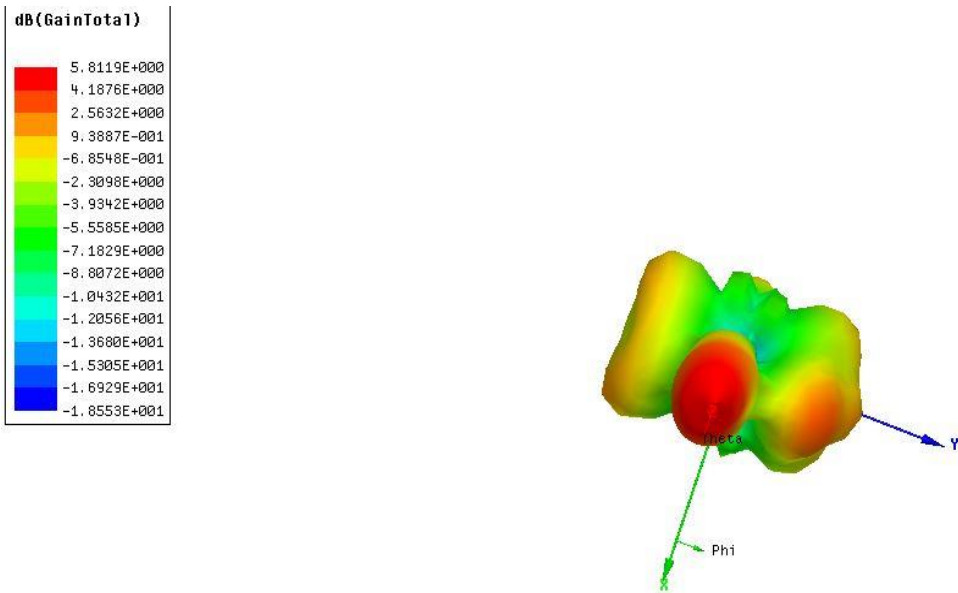


Figure 42:3D radiation pattern

**Table 4: Comparison Table**

PAPER	SIZE(mm by mm)	S11 (dB)	VSWR	GAIN	OPERATING BANDS(GHz)
[3]	30x38	-36	1.4	1.94	6
[5]	24.1x20.5	-17.6 to -18.5	-	10.25 to 12.12	5.2
[6]	12x12.5	-27	-	9.86	25.1 to 37.5
[9]	16x16	-31	-	7.44	26 to 40
[12]	30x38	-18 -50 -53	1.2 1.06 1.06	5	4.43 to 8.82
[13]	5.9x6.9	-47.21	-	6.03	19 to 36.6
[14]	8x8	-40.9	1.01	5.48	60
[15]	50x50	-26	1.2	6.09	6
[16]	20x20	-18.27	2.13	4.46	10.15
[17]	8.5x10	-24.92/-16/-11.6	1.1/1.4/1.7	1.07/4.07/3.1	13.6/22.12/28
Proposed 1	8x9	-22/-22/-19	1.3/1.3/1.9	5.7/1.8/2.7	10.5/26.1/50
Proposed 2	8x9	-15/-22/-27	1.1/1.9/1.1	5.8	21.6/26.1/50.5



## CHAPTER 5

### 5. EXPERIMENTAL RESULTS

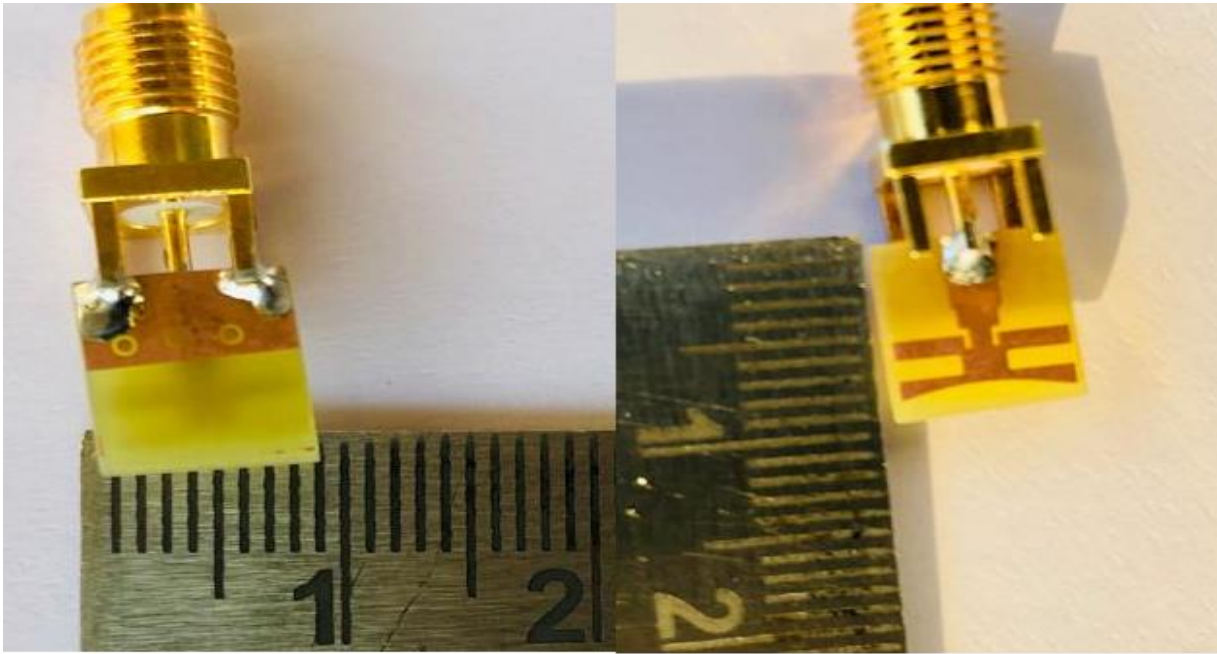


Figure 43: Actual Proposed Antenna

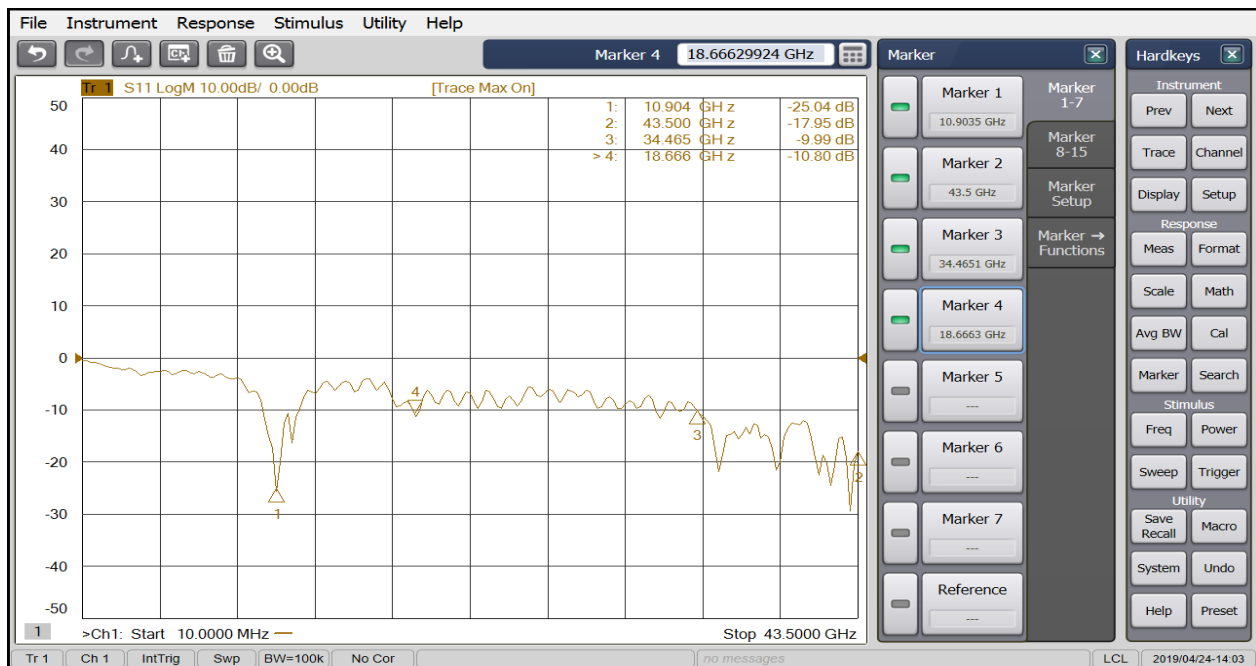


Figure 44:S11 measured on Network Analyzer

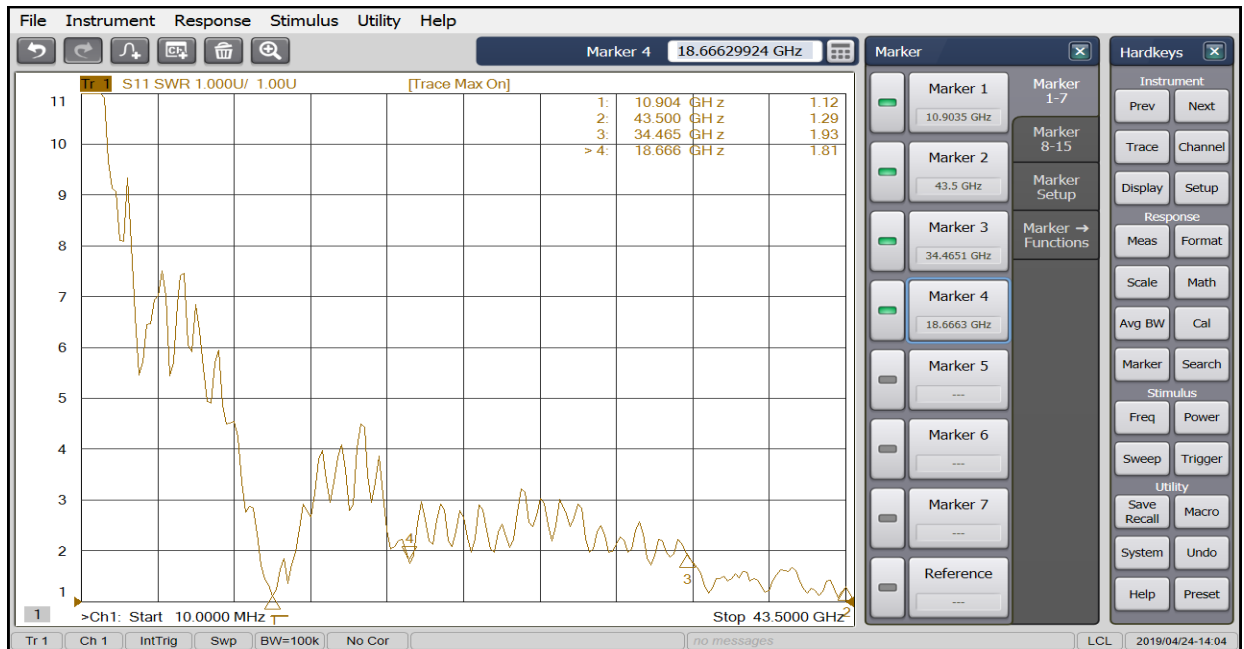


Figure 45: VSWR measured on Network analyzer

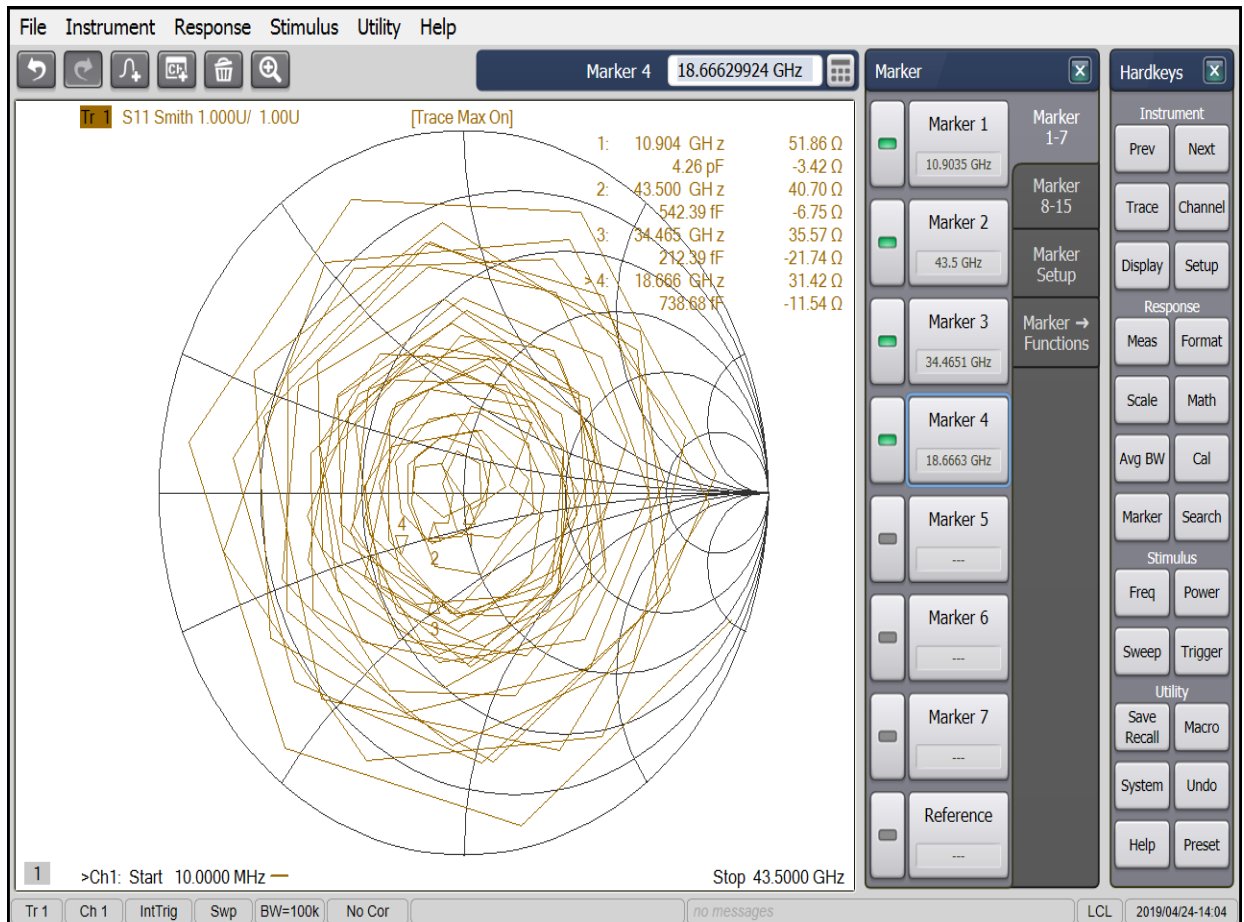


Figure 46: Smith chart measured on Network Analyzer

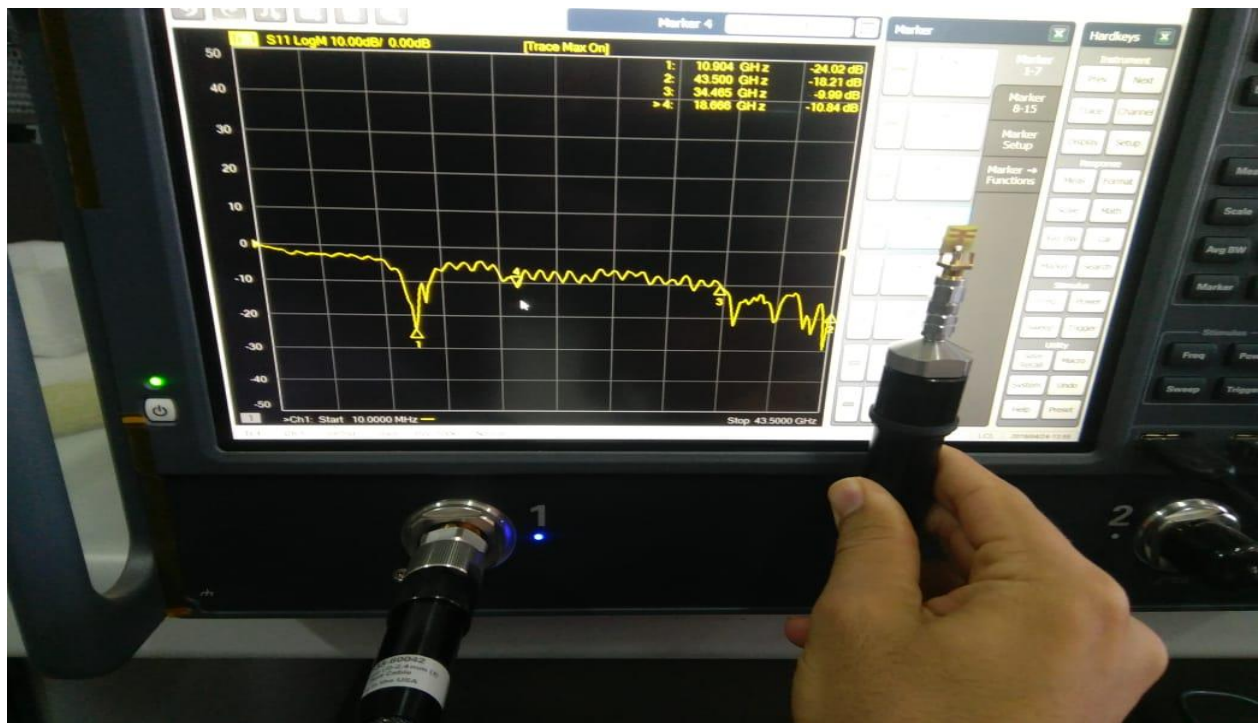


Figure 47: measured on Network Analyzer shown with antenna

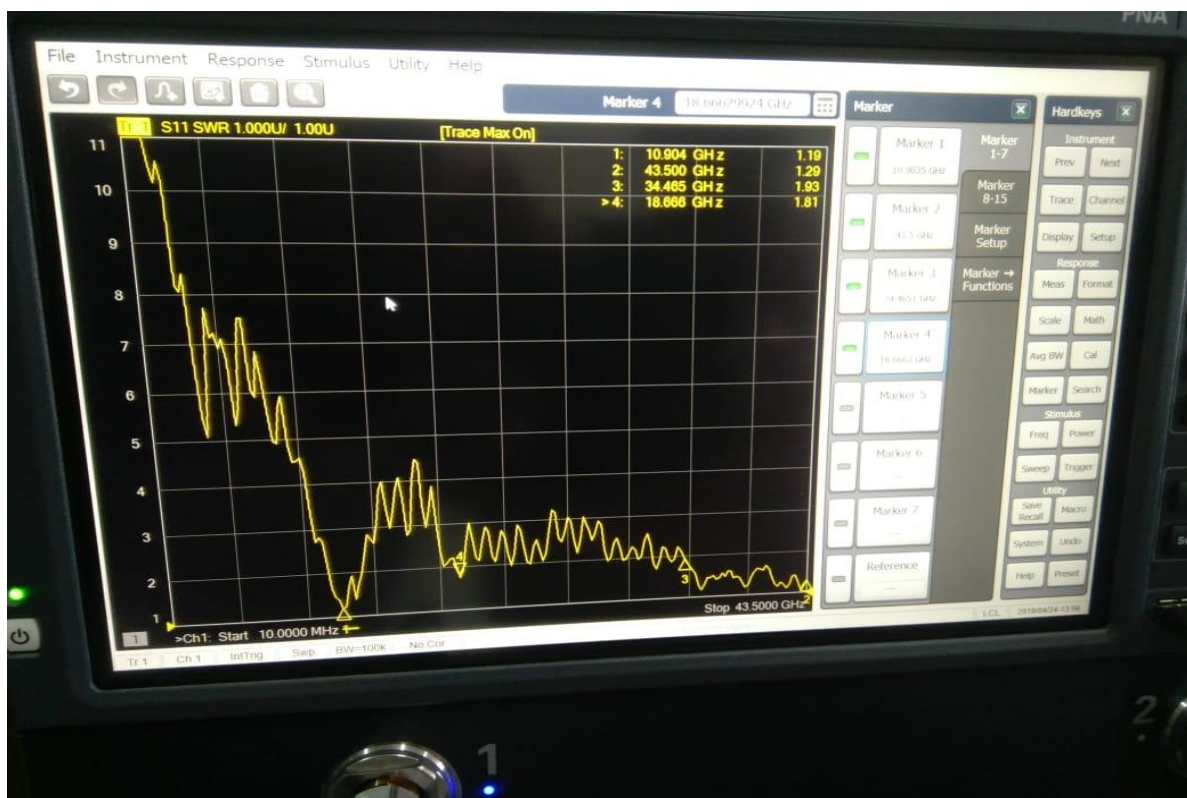
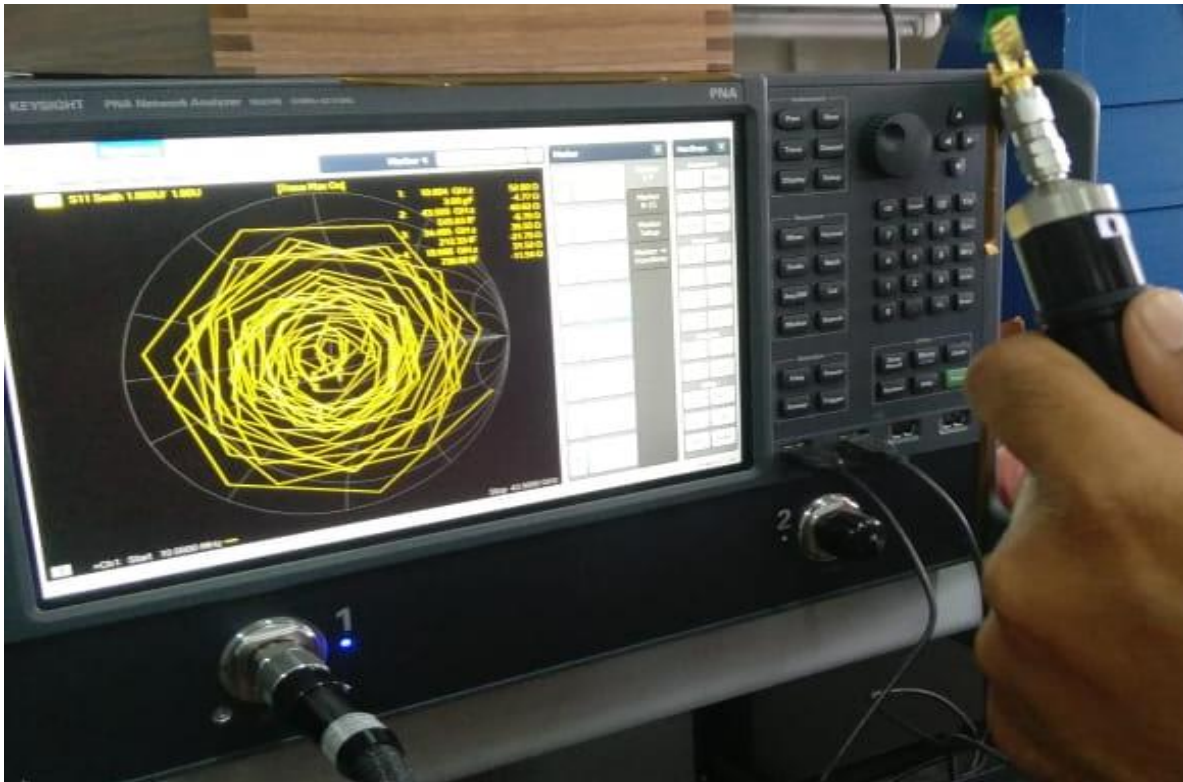


Figure 48: VSWR measured on Network analyzer shown with antenna



**Figure 49: Smith chart measured on Network Analyzer shown with antenna**

The fabricated antenna was tested in the DRDO Laboratory and the results obtained were even better than the simulated results as shown above. We observed a wide band for 5G from 34.5GHz to 50GHz.

For the fabricated antenna only the return loss, VWRS and smith chart are measured. Comparing it with the simulated results the experimental results are better.

## CHAPTER 6

### 6. CONCLUSION AND FUTURE WORK

The proposed antenna design makes use of multiple frequency bands and satisfies 5G operations for the frequencies 10.5GHz, 26.11GHz and 50.5GHz. The second design 21.6GHz, 25.5GHz and 50GHz. Because of its compact area, low weight and low cost of fabrication, the antenna is dependable for different portable devices for wireless applications and has improved performance. Validation of the simulation results is done by measurement thus satisfying the needs for 5G technology. This will enable timely availability of spectrum for mobile calls.

Further modifications can be made in the proposed design to make it more efficient for use in the near future.

Further alterations can be made in the proposed structure to make it increasingly productive for use sooner rather than later. In this design antenna is modified for better gain and performance in the frequency range of proposed 5G applications. The ground of the structure is modified to decrease the interference between the 5G system and other applications. The future of mobile communications is likely to be very different to that which we are used to today. While demand for mobile broadband will continue to increase, largely driven by ultra high definition video and better screens, we are already seeing the growing impact of the human possibilities of technology as the things around us become ever more connected. The upcoming 5th generation cellular network 5G is anticipated to exhibit a uniform Gbps data throughput experience across a vast range of user scenarios. Enabled by 5G, a programmable world will transform our lives, economy and society. Data throughput will be enhanced by more than a hundred fold.

The proposed antenna will be used for mm application of 5G, which can be placed at the top of the tower to be used for non-line of sight communications of 5G.



## 7. REFERENCES

1. R. G. S. Rao and R. Sai, *5G –Introduction & Future of Mobile Broadband Communication Redefined*. International Journal of Electronics, Communication & Instrumentation Engineering Research and Development (IJECIERD), vol/issue: 3(4), pp. 119–124, 2013.
2. G. Ancans, V. Bobrovs, G. Ivanovs, *Spectrum usage in mobile broadband communication systems*. Latvian Journal of Physics and Technical Sciences, 50 (3) (2013), pp. 49-58.
3. Youssef El Gholb , Mohamed El Bakkali , Ahmed Mounsef , Ikram Tabakh , Najiba El Amrani El Idrissi, *A 9-shaped antenna for 5G applications*. International Conference on Wireless Networks and Mobile Communications (WINCOM), 2017.
4. Rupali T. Lalpotu; T. D. Biradar; Sanjay Thakur, “*Improvement of bandwidth in printed monopole antenna by modified ground structures*”, International Conference on Global Trends in Signal Processing, Information Computing and Communication (ICGTSPICC) 2016.
5. M. Y. Chen et al., “*Conformal ink-jet printed C-band phased-array antenna incorporating carbon nanotube field-effect transistor based reconfigurable true-time delay lines*,” IEEE Trans. Microwave Theory Techniques, vol. 60, no. 1, pp. 179–184, 2012.
6. S. F. Jilani and A. Alomainy, “*Millimetre-wave T-shaped MIMO antenna with defected ground structures for 5G cellular networks*,” IET Microw. Antennas Propag., vol. 12, no. 5, pp. 672–677, 2018.
7. L.H. Weng, Y.C. Guo, X.W. Shi, and X.Q. Chen, “*An overview on defected ground structure*,” Progress In Electromagnetics Research B, vol. 7, pp. 173–189, 2008.
8. C. A. Balanis, “*Advanced Engineering Electromagnetics*”, United States of America: John Wiley and Sons, 1989.
9. Syeda Fizzah Jilani, Qammer H. Abbasi , Akram Alomainy, “*Inkjet-Printed Millimetre-Wave PET-Based Flexible Antenna for 5G Wireless Applications*”, IEEE MTT-S International Microwave Workshop Series on 5G Hardware and System Technologies (IMWS-5G), 2018.

10. T. S. Rappaport et al., “*Millimeter-wave mobile communications for 5G cellular: It will work!*,” IEEE Access, pp. 335–349, 2013.
11. S. Whitehead, “Adopting Wireless Machine-to-Machine Technology,” IEE Journal of Computing and Control Engineering, vol. 15, no. 5, pp. 40-46, Oct-Nov. 2004.
12. G. Wu, S. Talwar, K. Johnsson, N. Himayat, and K. Johnson, “M2M: From Mobile to Embedded Internet,” IEEE Commun. Mag., vol. 49, no. 4, pp. 36-43, Apr. 2011.
13. X. Li et al., “Smart Community: An Internet of Things Application,” IEEE Commun. Mag., vol. 49, no. 11, pp. 68-75, Nov. 2011.
14. Y. El Gholb, N. El Amrani El Idrissi, H. Ghennioui, « 5G: An Idea Whose Time Has Come” International Journal of Scientific & Engineering Research, Volume 8, Issue 3, March-2017.
15. Ban, Y.-L., S.-C. Sun, P.-P. Li, J. L.-W. Li, and K. Kang, “Compact eight-band frequency reconfigurable antenna for LTE/WWAN tablet computer applications,” IEEE Transactions on Antennas and Propagation, Vol. 62, No. 1, 471–475, Jan. 2014.
16. Hwang, S.-G., C. Yoon, I. S. Yoon, L. Chares, C. S. Park, and W.-S. Kim, “A reconfigurable mobile antenna for multiband operation using pin-diode,” Microwave and Optical Technology Letters, Vol. 57, No. 2, 406-409, Feb, 2015.
17. Zhang, P.-F., S.-Z. Liu, and S. Zhao, “A novel reconfigurable microstrip patch antenna with frequency and polarization diversities,” Microwave and Optical Technology Letters, Vol. 57, No. 6, 1494–1500, Jun. 2015.
18. Xia Xiao, Wei-Hua Zong, Shan-Dong Li, Xiang-Yang Wei, and XiaoYun Qu “A Wideband Slot Antenna for Mobile Phone Applications”, IEEE 5th Asia-Pacific Conference on Antennas and Propagation (APCAP), 2016.
19. Jui-Han Lu, Jia-Ling Guo and Yong-Yong Zhang<sup>[1]</sup> “Planar Multi-Band LTE/WWAN Antenna for Internal Mobile Phone”, 5th IEEE AsiaPacific Conference on Antennas and Propagation (APCAP) , 2016.
20. Pozar, D. M., “Microstrip antenna,” IEEE Proceedings, Vol. 80, 79–81, Jan. 1992.

21. C. A. Balanis, *Advanced Engineering Electromagnetics*. United States of America: John Wiley & Sons, 1989.
22. Herscovici, N., "A wide band single layer patch antenna," *IEEE Trans. on Antenna and Propagations*, Vol. 46, No. 4, 471–474, April 1998.
23. Chen, Z. N., "Broadband probe-fed L-shaped plate antenna," *Microwave and Optical Letters*, Aug. 2000.
24. T. Rappaport et al., "Millimeter Wave Mobile Communications for 5G Cellular: It Will Work!," *IEEE Access*, vol. 1, May 2013, pp. 335–49. [15] T. S. Rappaport et al., "Broadband millimeter-wave propagation measurements and models using adaptive-beam antennas for outdoor urban cellular communications," *IEEE Trans. Antennas Propag.*, vol. 61, no. 4, pp. 1850–1859, Apr. 2013